

Development of the Robotic Touch foot Sensor for 2D walking
Robot, for Studying Rough Terrain Locomotion

By

HUNWOO LEE

Submitted to the graduate degree program in Mechanical Engineering and the
Graduate Faculty of the University of Kansas in partial fulfillment of the
requirements for the degree of Master of Science.

Chairperson Dr. Terry Faddis

Professor Dr. Bedru Yimer

Professor Robert Umholtz

Date Defended: June 5, 2012

The Thesis Committee for HUNWOO LEE
certifies that this is the approved version of the following thesis:

Development of the Robotic Touch Foot Sensor for 2D Walking Robot, for Studying
Rough Terrain Locomotion

Chairperson Dr. Terry Faddis

Date Accepted: July 6, 2012

Abstract

Many researchers have been developing biped walking robots with excellent techniques and advanced technologies. However, ordinary locomotion is executed on even terrain such as flat surface. This means that many researches are focusing much on image processing, programing techniques and newly suggested devices, but not much research is being done on the proper sensors to robotic feet. Regarding robot gaits on unknown ground, one of the most significant determinations is to investigate balance by itself.

A new sensor was studied for the robotic foot in order to allow walking on rough ground by sensing variations in the pressure profile on the foot. The primary purpose of this study is to provide a proper foot sensor for Jaywalker. The Jaywalker has been developed by the Intelligent Systems and Automation Laboratory. Jaywalker provides a good platform for the study of rough terrain walking. The sensor to be developed for the robot must be applicable to every structure and flexible and able to impulsive forces, as well as having a reasonable manufacturing cost.

The main concept of this new type of sensor is to utilize the special application and design of inductive touch sensors. The Propeller microprocessor plays an important role in the control of the new sensor. The results of this study indicate that the new inductive sensor can be useful as a robotic foot sensor for the study of rough terrain walking.

Acknowledgments

I would like to thank my advisor, Dr. Terry N. Faddis, for his guidance and support while doing this study. I would also like to thank my committee members, Dr. Bedru Yimer and Professor Robert C. Umholtz for their support throughout this research.

Finally, I would like to thank my family, Mr. Janggun Jo, Preston White and Hyunki Lee, whose support has been vital to my work. Especially, I would like to thank Gavin Strunk, since we have shared many things in common, while he helped me in many ways. In addition, I would like to express my great thank to Professor Peter Chun as my spiritual teacher who is the Professor of Viola in the School of Music at KU. I would like to give special thanks to my wife and son, for their sacrifice and support. I know the difficulties you have gone through, as dependents of an international student. I will serve and sacrifice for you more back home in Korea.

Lastly, I would like to remind myself of my nation and people, who provided this opportunity. Lastly, thank you, God, for letting me study and live in the most wonderful country in the world for two years.

With deep gratitude,

Hunwoo Lee

Table of Contents

LIST OF FIGURES.....	vii
NOMENCLATURE.....	ix
INTRODUCTION.....	1
1. Basic theories related to robotic touch foot sensor.....	6
1.1 The advantage of the inductive touch sensor	6
1.2 Basic theories involved in the robotic touch foot sensor.....	9
1.3 Analysis of maximum impact power.....	12
2. IMPLEMENTATION OF THE ROBOTIC TOUCH FOOT SENSOR	14
2.1 Making coil flat and spiral.....	14
2.2 Current generator.....	17
2.3 Passive low pass filter.....	19
2.4 Analog to Digital conversion with a sampling clock generator.....	19
2.5 Power management and avoiding redundancy with multiplexers.....	21
2.6 Microprocessor to read ADC	23
2.7 Test beds for developed sensors.....	23
3. Trouble shoots.....	25
3.1 Interference among coils.....	25
4. Test and results.....	27
4.1 Coil tests.....	27
4.2 Measurement of each coil.....	27
CONCLUSIONS AND RECOMMENDATIONS.....	32
APPENDIX A: Flowchart of the robotic touch foot sensor	1
APPENDIX B: Schematics for the robotic touch foot sensor circuits.....	2
B.1: The first circuit for the robotic touch foot sensor.....	2
B.2: The second version of the sensor circuit.....	3
B.3: 1 MHz vibrator to NPN Transistor.....	4
B.4: 4 MHz vibrator to ADC	5
B.5: Diagram for 4 coils with 2 multiplexers.....	6
B.6: Wiring diagram for ADC setup to microprocessor	7
B.7: Wiring diagram for excited current driver with a multiplexer.....	8
B.8: Wiring diagram for test bed	9
APPENDIX C: Interference among coils	10
C.1: The first test about mutual interference at the beginning	10
C.2: The second test for interference.....	12

APPENDIX D: Programing code for robotic touch foot sensor working.....13

APPENDIX E: Characteristics of coils.....18

List of Figures

Figure 1: Advanced characteristics of new ASIMO	2
Figure 2: Structure of prototype of tactile sensor foot	2
Figure 3: Jaywalker studied in ISAL.....	3
Figure 4: Keypad of Inductive touch sensor	5
Figure 5: Cross-sectional view of an inductive touch sensor.....	6
Figure 6: Example about Eddy Currents.....	7
Figure 7: Outer structure of the inductive touch sensor.....	8
Figure 8: Basic RLC circuit diagram	9
Figure 9: Serial RLC circuit from Wikimedia.....	10
Figure 10: Coil diagram from side view.....	11
Figure 11: Phase diagram for low pass filter and simple circuit for low pass filter...12	
Figure 12: Simulation of maximum impact force on the steel using Adam's program.....	13
Figure 13: Plot on wood maximum impact force.....	13
Figure 14: Test procedure for the sensor.....	14
Figure 15: Making a spiral coil with new material.....	15
Figure 16: Drawing of a coil for PCB.....	16
Figure 17: Four etched coils on PCB.....	17
Figure 18: Timer 555.....	17
Figure 19: Devices for current generator circuit.....	18
Figure 20: Devices to be used for analog to Digital conversion.....	20
Figure 21: Multiplexer.....	21
Figure 22: Multiplexer to power source.....	22
Figure 23: Multiplexer (d) to ADC (b)	22
Figure 24: Sandal with coils as a test bed.....	24
Figure 25: A measurement tool for coil.....	28
Figure 26: The characteristic curve of the hand-made coil of voltage to depth.....	29
Figure 27: Curves to 4 hand-made coils with 13 turns wound to be set up on sandal(1st test bed)	29
Figure 28: 4 coils etched on PCB after removing interference.....	30
Figure 29: PCB Cover (P) is added to the previous setup.....	31
Figure A.1: Flowchart of the robotic touch foot sensor.....	1
Figure B.1: The first circuit to test sensors without selecting one of sensors.....	2
Figure B.2: The 2nd circuit to solve power consumption with a multiplexer.....	3
Figure B.3: 1 MHz multi-vibrator to make NPN transistor oscillated with required current.....	4
Figure B.4: 7 MHz multi-vibrator to be used for ADC as sampling clock.....	5

Figure B.5: Wiring diagram between Op-Amp and multiplexers connected to input of ADC.....	6
Figure B.6: Wiring diagram for ADC to micro controller and the output of 4 Op Amps.....	7
Figure B.7: Clock generator with a current driver and multiplexer to separate one coil from others against interference.....	8
Figure B.8: Test board for various experiments.....	9
Figure C.1: Setup wiring diagram for testing.....	10
Figure C.1.1: pictures above shows how to conduct the test.....	11
Figure C.2.1: Testing interference among coils. The circuit diagram is Introduced in Appendix B.2.....	12
Figure E.1 4: curves from table E (a)	19
Figure E.1 4: curves from table E (b)	20

Nomenclature

ACK	Acknowledge
ADC	Analog/Digital Converter
AIT	Acknowledge In Turn
ANN	Artificial Neural Network
CAD	Computer Aided Design
CAN	Controller Area Network
CNS	Central Nervous System
CPU	Central Processing Unit
DB-25	D-Subminiature 25 Pin
DIP	Dual Inline Package
DSP	Digital Signal Processor
EBUS	Emergency Bus
EEPROM	Electrically Erasable Programmable Read Only Memory
FPGA	Field Programmable Gate Array
GPIO	General Purpose Input/Output
GUI	Graphical User Interface
HPA	High Priority ACK
HPAA	Hybrid Parallel Ankle Actuator
I ² C	Inter-Integrated Circuit
iHD	Independent Hip Drive
IPM	Inverted Pendulum Model
KB	KiloByte
LCD	Liquid Crystal Display
LEGS	Leg Extension Guidance System
MEMS	Microelectromechanical Systems
MHz	Mega Hertz
MIMD	Multiple Instruction Multiple Data
MISD	Multiple Instruction Single Data
MMPS	Multi-Master Parallel Slave
MSB	Most Significant Bit
PCB	Printed Circuit Board
PD	Proportional Derivative
PWM	Pulse Width Modulation
RAM	Random Access Memory
ROM	Read Only Memory
SCL	Serial Clock Line
SD	Secure Digital
SDA	Serial Data Line
SIMD	Single Instruction Multiple Data
SPI	Serial Peripheral Interface
VDC	Voltage Direct Current
VGA	Video Graphics Array
VM	Virtual Model
ZMP	Zero Moment Point

Introduction

Many researchers have been working hard to make robotic movements to imitate human motion all over the world. Results of that effort are seen with robots now being able to accomplish tasks that were once performed solely human workers such as in factories, like automobile industries and electronic circuitry production lines.

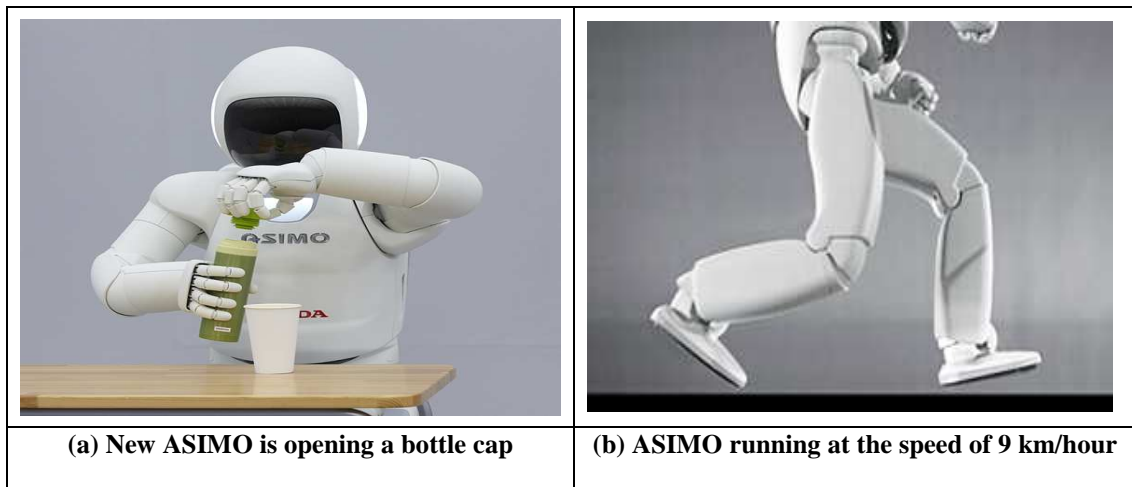
Now days we have also witnessed that cleaning robots are vacuuming and wiping floors from advertisements on TV or markets. For military applications, General Dynamics Co made the “Big dog” robot and showed it how to walk on rough ground and icy floor. Big dog can control its balance even when it gets pushed by a man. Thus, it is true that robots are getting more integrated into our daily lives as well as military operations. A few months ago, Honda Co presented a new model of robot, ASIMO, which can open a cap of a water bottle and run at a certain speed as shown in Figure1. Its movement and walking show advanced technology of robotics. Below are the major enhanced properties to the old version.

Table 1. Remarks to enhanced properties of the new model to the previous one [1]

1. Height	130 cm
2. Weight	48kg (decreased 6kg from previous model)
3. Operating degrees of freedom(DOF)	Total: 57 degrees of freedom (increase of 23 degrees of freedom from previous model)
4. Running speed	9km/hour (previous model: 6km/hour)

The new video of ASIMO is enough to encourage researchers to have interest in that area [1]. It recognized different types of objects by image processing and controlled its arms and legs more like humans do. So ASIMO demonstrates bi-pedal robotic walking is quite well-developed on the even ground or stairs, but there are many other areas to be enhanced for making it more fully

humanized. When taking a close look at ASIMO's sensors, it has a 6 axis-force and-torque sensor, according to its guidebook published by Honda Co [1]. That sensor is mounted on each joint in order to sense torque, force and direction. That helps control ASIMO while running and walking at varied speed as well as keeping its balance [1].



(a) New ASIMO is opening a bottle cap

(b) ASIMO running at the speed of 9 km/hour

Figure 1. Advanced characteristics of New ASIMO, Demonstration video for the new ASIMO: <http://www.youtube.com/watch?v=LuymCZL5aWM>

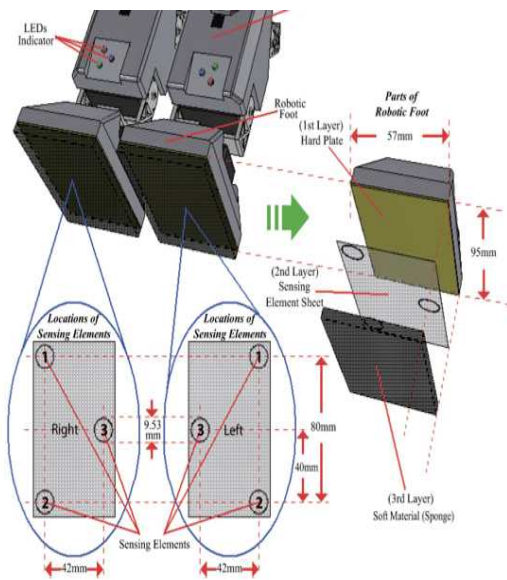


Figure 2 structure of prototype of tactile sensor foot [2]. ①, ②, ③ are Flexi Force resistors. These 3 points sense the bottom

However, as always it is still walking on even ground with its flat and big feet.

Another interesting article related to the sensor for robot's foot is the haptic robotic sensor that can sense 4 different ramped grounds [2]. This task is accomplished by using 3 sensing points per foot so that it keeps balanced based on the

combined conditions of sensed inputs from them as shown in figure 2 [2]. The ramps can be sensed by "Flexi Force"

(manufactured by Tekscan Inc) which is a sort of resister to respond to force [2]. When it comes to heavy and rough walking loads, that sensor is not robust enough against weariness and sudden impact. Still, it is the result of a decent research on a small humanoid robot showing how to control balancing problem, but lacks the ability to sustain continual abuse without degrading over time.

Checking the state of various parameters of a robotic foot is vitally important to the control of walking and balance. That is why the Intelligent Systems and Automation Laboratory (ISAL) has been focusing on this matter. Successive graduate students have enhanced “Jaywalker,” a three legged robot developed to study rough terrain walking, in the sagittal plane, shown in figure 3. The necessity of new types of sensory information on the foot was echoed by the thesis on ‘Parallelized Distributed Embedded Control System for Two Dimensional Walking Robot for Studying Rough Terrain’ [3].



(a) side view of JayWalker



(b) Front view

Figure 3. Jaywalker studied in ISA Lab

(‘Jaywalker’ is a three legged, two-dimensional biped walking robot. It is used as a test bed to study rough and unstructured ground locomotion. 2D walking is carried out by coupling the two outside legs together, so the robot appears to have two legs when looking from a side view.)

The purpose of my research is to develop a possible sensing method for rough and unstructured terrain, with resistance against wear and impact force. This sensor will be referred to as the 'Robotic touch foot sensor'. To this end, it is imperative for the new sensor for a robotic foot to endure much sudden impact force, not to be worn out by many contacts and to give us stable outputs proportional to inputs. In addition, it is necessary for the sensors to resist water or other liquids. To accomplish this purpose, there are many and various types of sensors can be utilized: mechanical switches, lasers, ultrasonic sensors, piezoelectric sensors, and inductive touch sensors.

Among the sensor choices, switches were considered first. A switch is used to produce one or zero based on inputs in a mechanical way. This is an easy method to use, and inexpensive, but causes mechanical noise, in addition to wearing out and prone to physical deformation. Secondly, lasers are commonly used for measuring distance, however it is difficult to find a laser in a small package, includes driving circuitry, and is capable of enduring unexpected shock. Lasers tend to be expensive relative to other sensor options, and a receiver may interpret signals from adjacent lasers due to reflection on uneven surfaces. Following the lasers is the ultrasonic sensor. This sensor cannot read the status of ground under grass or other objects. In addition, the angle of the ankle would cause scatter of the signals reflected against the ground while walking. The ultrasonic sensor is better used for recognition of objects and path planning. The next sensor that would be possible for the robotic foot is a piezoelectric sensor. Piezoelectric sensors basically operate by producing a voltage due to physical displacement. Its disadvantage is that it cannot endure resistance against liquid material. This type of sensor is one of the most applicable sensors to a robotic foot sensor and would have been a potentially viable option with weather proofing that did not adversely affect its performance. The inductive touch sensor was pursued due to its advantages over the previous. The Microchip Company first introduced its new inductive sensing product in 2009 [4]. This technology, shown in figure 4, was used to design a keyboard (or pad)

for the special purpose of use under water or in harsh environments [4]. The idea is that the new keypad uses the varied inductance of a flat coil, which radiates electromagnetic field perpendicular to the coil, by cutting off magnetic fields [4]. The electromagnetic field is varied by a piece of metal at various distances to the coil [4].



Figure 4. Keypad of Inductive touch sensor [4]

The ability to put a flexible material as a gap layer between metal and a coil allows the sensor to absorb strong impacts caused by walking with fast response to the changing pressures. In addition, the sensor is not degraded by numerous touches due to indirect sensing. For these reasons, the inductive touch sensor is able to meet the design requirements of the Jaywalker better than the other sensors.

My thesis is organized as follows. The first chapter introduces the basic theories about the touch sensor in detail including the signal amplification and digital conversion to provide a readable output. Chapter 2 presents the implementation with problems and solutions at each step. Next, troubleshooting is introduced in chapter 3. And then tests and results are provided in chapter 4. In chapter 5, I discuss the results and offer recommendations to future researchers who continue to work on this area.

I. Basic theories related to the robotic touch foot sensor

1.1 The advantage of the inductive touch sensor

A difficulty when designing switches and touch screen panels for harsh environments using capacitive or resistive touch technologies is they cannot be put into water. The inductive touch sensor can work under water or under specific environments like freezing weather so that allows people to utilize keypads for the electronic devices used in these environments [4].

The way to operate an inductive sensor is an important foundation for this study on robotic foot sensor. The general principle is from the electromagnetic fields that are created by a coil.

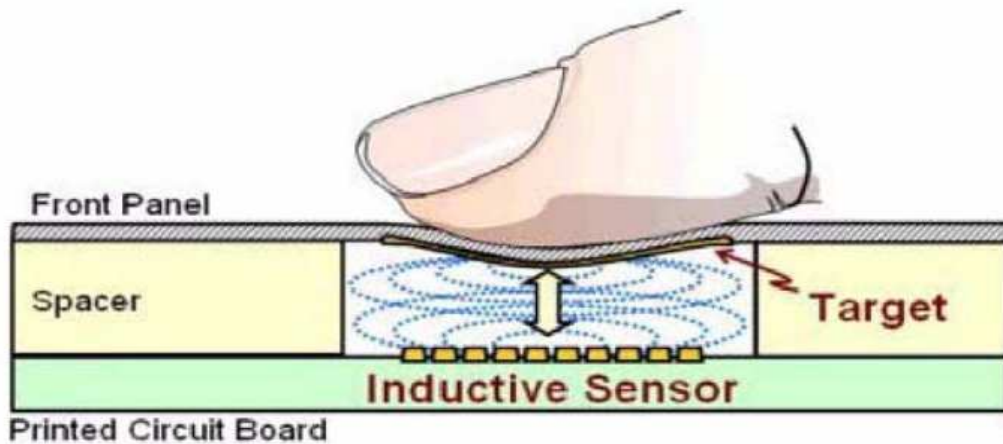


Figure 5. Cross-sectional view of an inductive touch sensor [4]

As shown in figure 5, the coil in the form of spiral is excited with the pulsed current. The pulsed current causes magnetic flux in the perpendicular direction to it. With the electromagnetic fields, conductive metal like copper or silver decouples them. The decoupled flux keeps the positive magnetic radiation from increasing. This phenomenon can be explained by the eddy current, as shown in figure 6. An application of the inductive sensor is, Eddy Current Non-Destructive Testing (NDT), for testing a surface of metal for cracks or it can pick up flaws like uneven and varied thickness coatings [5]. The Eddy Current induces electric currents in a conductor when it is

put into a varying magnetic fields [6]. Historically, eddy current was discovered by François Arago in 1824, and described by Maxwell Faraday. In 1879, David E. Hughes initially used the principle for Non-Destructive Testing (NDT) to execute tests for quality of metal products [5].

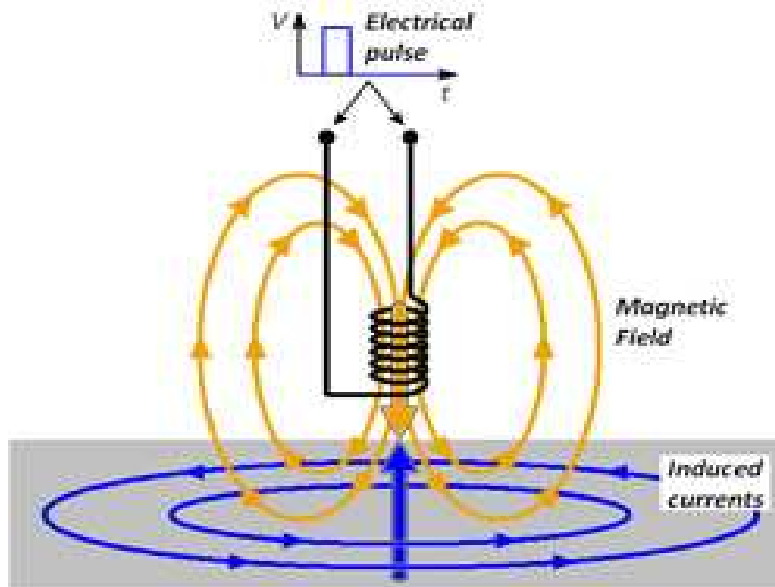


Figure 6. Example about Eddy Currents
http://www.pecscan.ca/imgs/driving_coil.jpg

As shown in figure 6 above, the current generated by excited coil causes swirling currents on the conductor [6]. The eddy current also creates its own magnetic fields (Blue arrow) against the origin (Yellow arrow) [6]. As such, the magnetic fields are decoupled with the induced flux [6]. It ends up with reducing the inductance of the coil. In other words, based on this distinct current, the closer the gap between coil and metal, the more flux gets decoupled. The inductance is decreased, so the voltage across the coil is also reduced. In this manner, detected voltage difference in the coil is going to be handled as data and converting it to digital is followed [4].

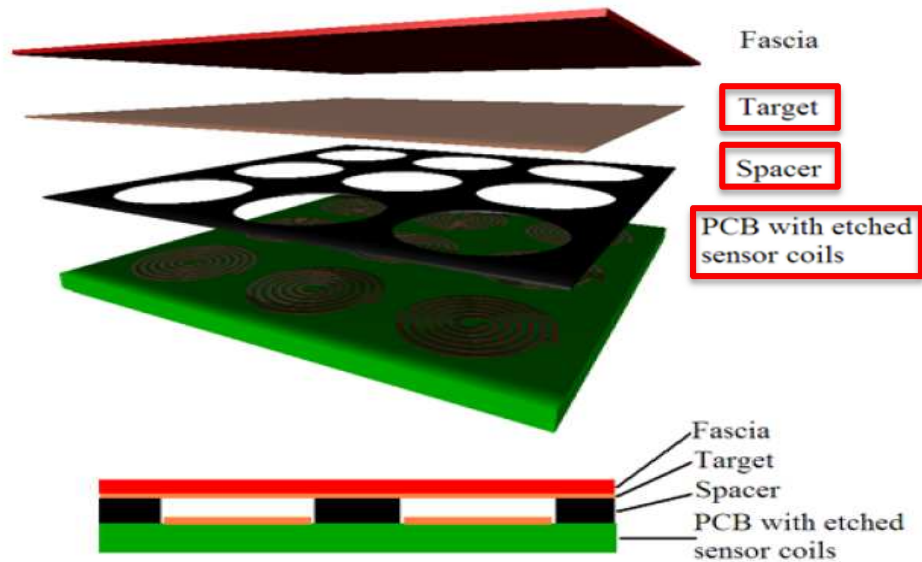


Figure 7. Outer structure of the inductive touch sensor [4]

The physical design to be implemented on the product, as shown in figure 7, consists of 3 components: one is the “target”, another the “spacer”, and the other the “coil” [4]. The metal, which is called the “target”, makes electromagnetic fields change by cutting them off, causing the voltage across the coil to become lower or higher, depending on how close the target is located from the coil. The shape of the coil from the side view is flat. There is a space between the coil and a target. The layer between them is referred to as the gap spacer. This spacer will determine how much force is required to be deformed to a certain point when pressed. This space can also be filled with other insulated materials; air, rubber, urethane, etc. The property of a spacer can be adjusted by replacing the material or changing thickness of it. It depends on conditions of a system as to what material selection is appropriate. Therefore, this type of sensor can transfer the status about bottom of robotic foot to the system and provide a feasible method to develop a well-functioning robotic foot.

1.2 Basic theories involved in the robotic touch foot sensor

Basically, there are 4 parts to be described in the foot sensor. The first is a multi-vibrator circuit to activate the coil with pulsed current. The next, is the detecting area with a coil amplified and filtered through an Op amp and a low pass filter. The next is how to digitize the detected signal. Finally, the microprocessors used for the implementation will be described.

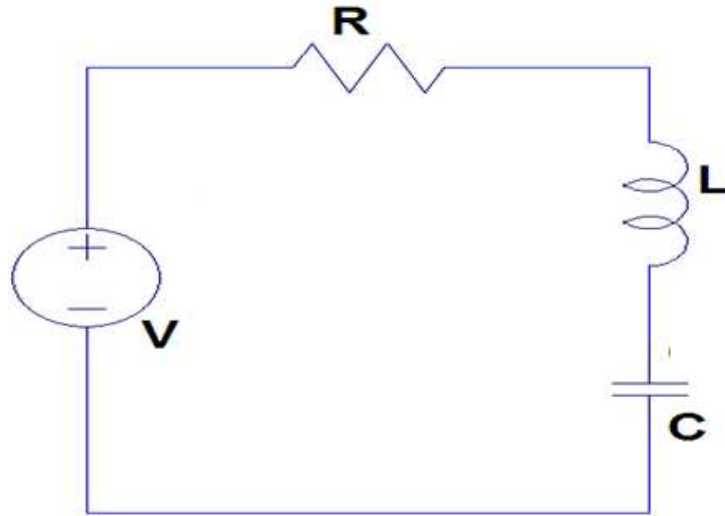


Figure 8. Basic RLC circuit diagram. ‘V’ runs with oscillation of a certain frequency

Above all, the coil needs an oscillating source to be excited. In the AC circuit, shown in figure 8, R is resistance, L inductance and C conductance. With an oscillating input, the inductance and conductance are varied to the frequency in accordance with circuit theory.

$$Z_L = \frac{V(t)}{i(t)} = j\omega L = j(2\pi fL), \quad V(t) = L \frac{d\{i(t)\}}{dt} \quad (1)$$

Therefore, the voltage across the coil from equation (1) is proportional to the value of L. At a fixed frequency, the voltage across inductor is related to the ratio of the inductance to total impedance [7, 8].

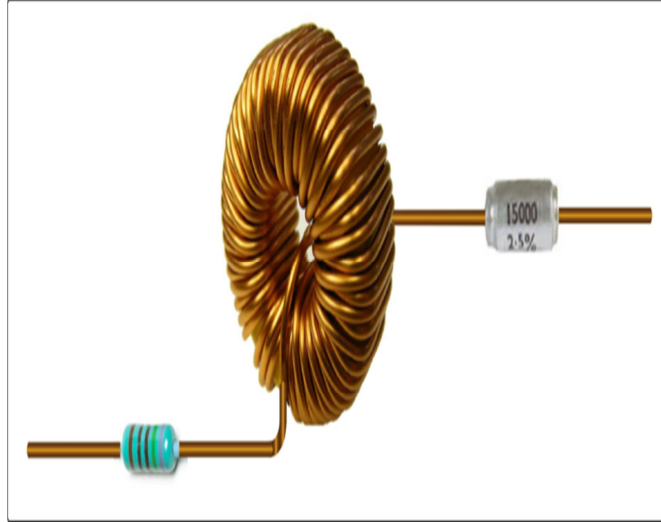


Figure 9 Serial RLC circuit from Wikimedia
[http://upload.wikimedia.org/wikipedia/commons/4/4e/RLC_series_circuit.png]

The inductance goes down as the metal gets closer and results in a voltage drop. In this way, the inductive touch sensor can read the varied position of target metal. The intensity of L is proportional to the number of windings in the coil and the width of the trace [8, 9]. A typical inductive coil is shown in figure 9. For my investigation I developed a flat coil, as shown in figure 17. This shape is extraordinarily different from the typical inductive coil. When current is applied to flat coil, electromagnetic fields occur which are perpendicular to the plate surface by the right-hand rule [9]. This calculation follows the formula which is shown below [10].

$$L = \frac{N^2 \times A^2}{30A - 11 D_1} \quad (2)$$

$$A = \frac{D_1 + N(W+S)}{2} \quad (3)$$

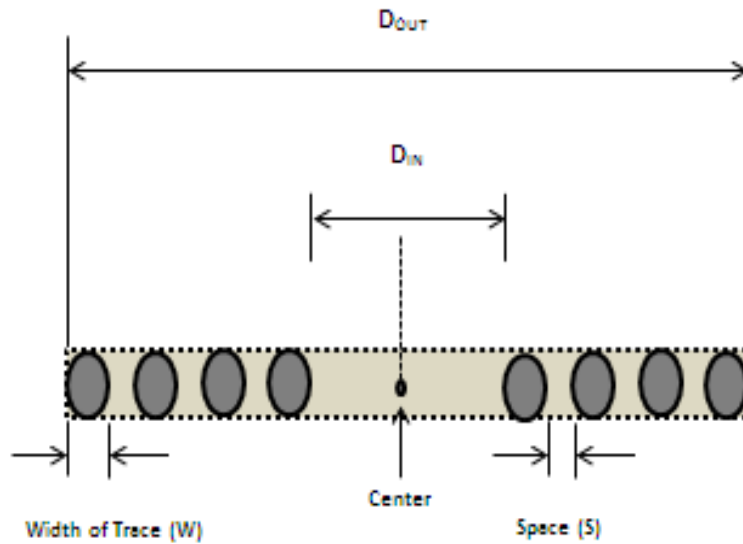


Figure 10. Coil diagram from side view

In chapter 2, it will be brought up again to discuss the actual coil value.

An Operational Amplifier (Op amp) is used to amplify the detected signal.

To clean signals against noise or make them smooth, low pass filter, high pass filter and band pass filter are the applicable ways to do that [8]. Low pass filter passes low frequency signals, but attenuates signals with frequencies higher than the cutoff frequency.

A high-pass filter is the opposite of a low pass filter. A band pass filter is a combination of a low-pass and a high-pass filter.

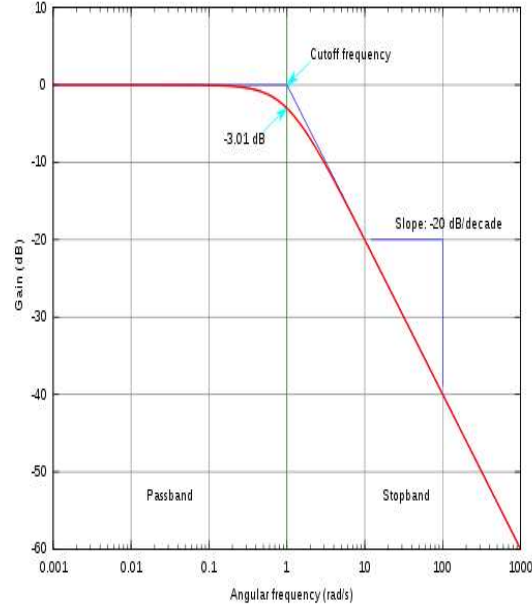
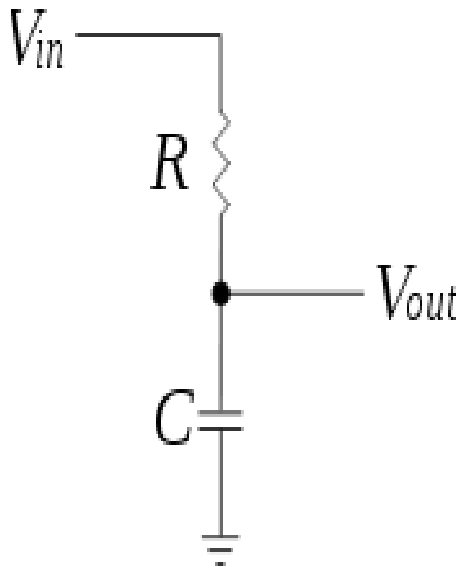
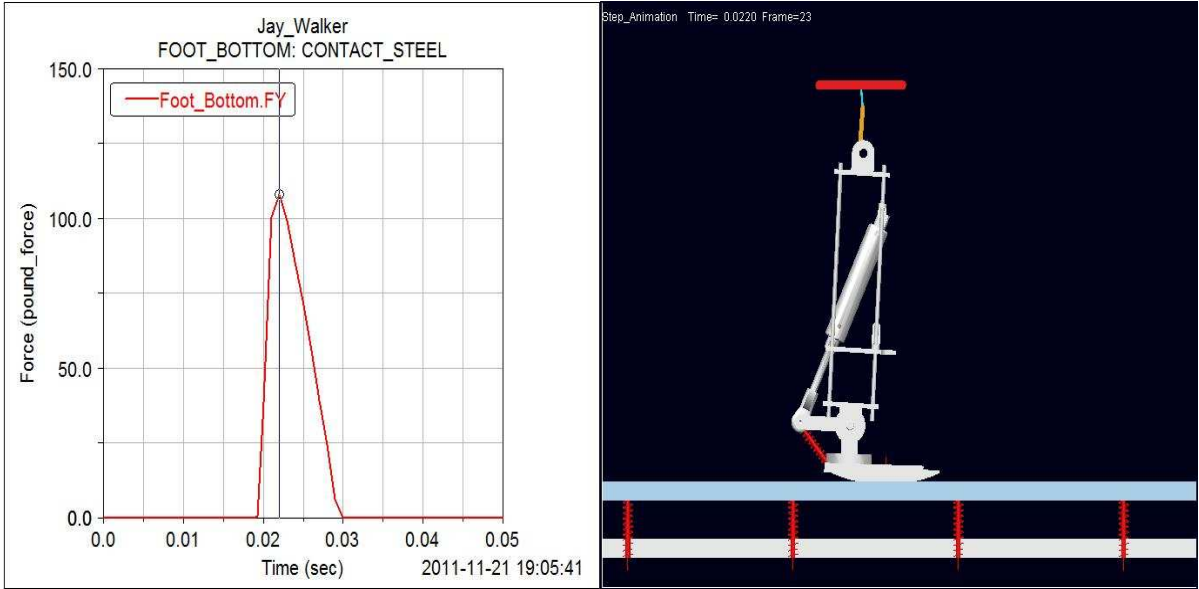


Figure 11 (a) Phase diagram for Low pass filter (b) simple circuit for Low pass filter from WIKIPEDIA, http://en.wikipedia.org/wiki/File:RC_Divider.svg

Figure 12, it is a simple low pass filter that was used in this work. After the data comes out of the low pass filter, they are converted from the analog to digital form

1.3 Analysis of maximum impact force

The thickness and stiffness of elastic layer must be carefully selected for the sensor on the robotic foot. In order to do that, the maximum force on the bottom of the foot should be estimated while the robot (Jaywalker) is taking a step. During the fall semester of 2011, Preston White, who is an applicant for the Master’s degree in ISAL, simulated forces of Jaywalker, with the ADAMS program [Appendix 15]. The impact expected on the different ground conditions is calculated by his analysis. In accordance with his report, the maximum impact force is calculated to 108 lb-force (lb-f) on steel and 106.5 lb-f on wood. Figures 13 and 14 below are the plots from the simulation. As a result, 108 lb-f was the reference for the induction sensor spacer with relation to distance.



(a) Plot on the steel floor

(b) simulated JayWalker on ADAMS program

Figure 12. Simulation of maximum impact force on the steel ground using Adam's program

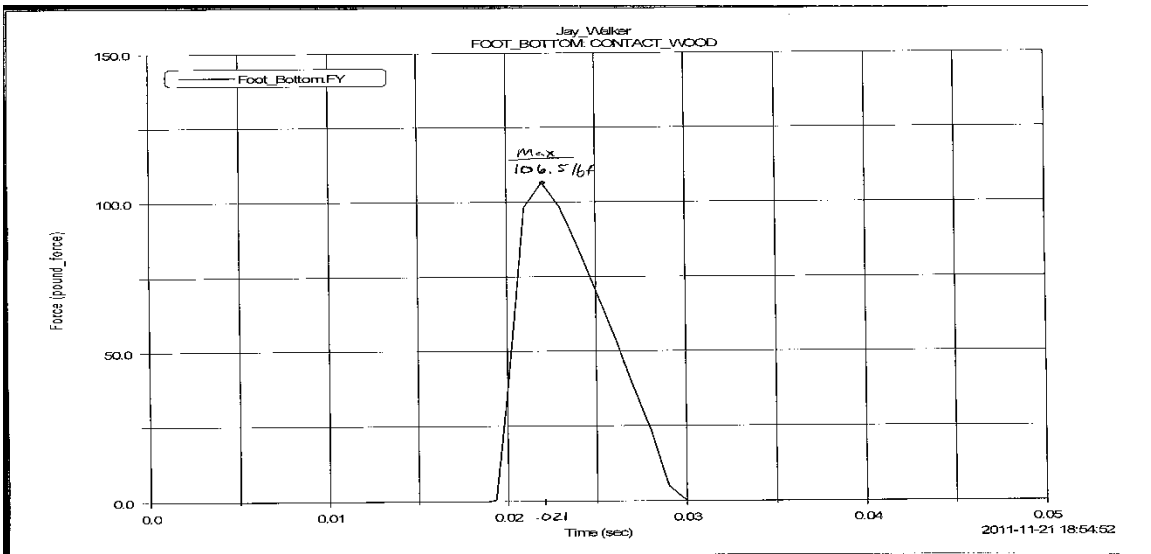


Figure 13. Plot on the wood ground maximum impact force

Chapter 2. Implementation of the robotic touch foot sensor

The flow diagram in figure 15 below, is an overview of process to make one sensor read with a microprocessor. The critical process is to design the circuit for the sensor to reliably detect varied inductance and therefore varied force.

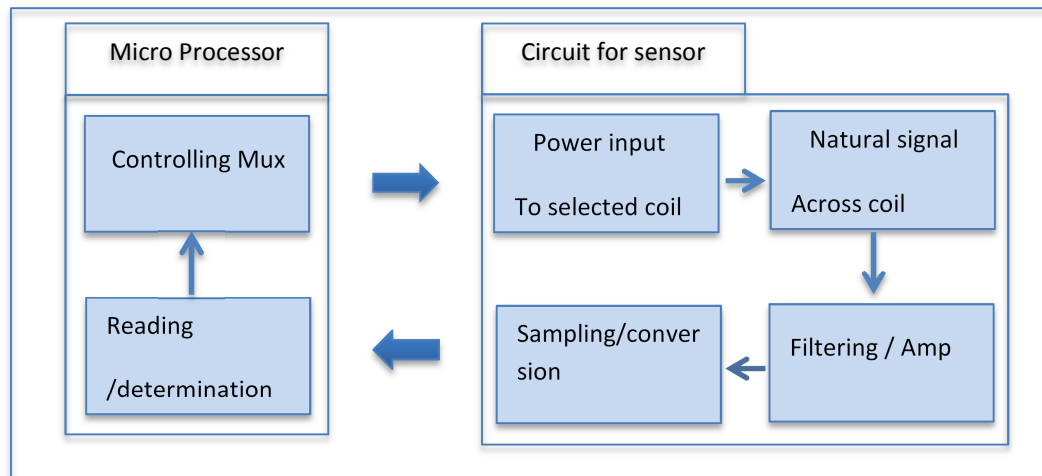
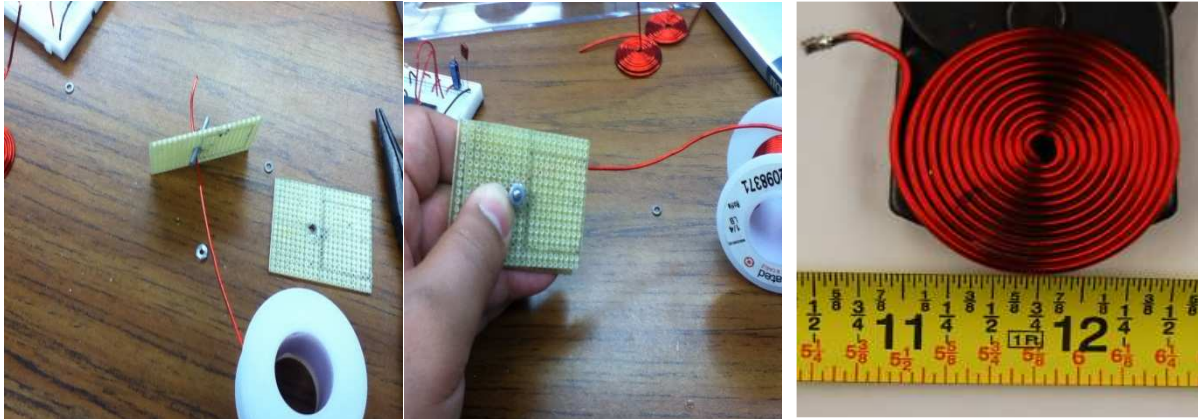


Figure 14. Test procedure for the sensor

2.1 Making coil flat and spiral

To start with, a coil must be developed in a spiral and flat form on a Printed Circuit Board (PCB). Hand-made coils were developed for the initial experiment. The initial rectangular shaped coil was wound with 4 turns and non-insulated wire. In this test, the output from the plate deflection was from 281.3 mV to 375 mV. The difference was only about 93.7 mV. Next, a spiral shaped coil of 8 turns without insulation was tested and produced a better amplitude from 181.1mV to 412.2 mV with the same deflection. A problem with the test was that coils used were not insulated. An insulated coil with 8 turns gave higher voltages from 539.8mV to 1.401V, than those of non-insulated ones. The difference is about 807mV. Based on the experiments, a

magnetic wire was selected which had polyurethane and polyamide (nylon) insulation, was 0.052 inches in diameter, manufactured by Consolidated Electronic Wire & Cable Co.



(a) Inserting wire into plate

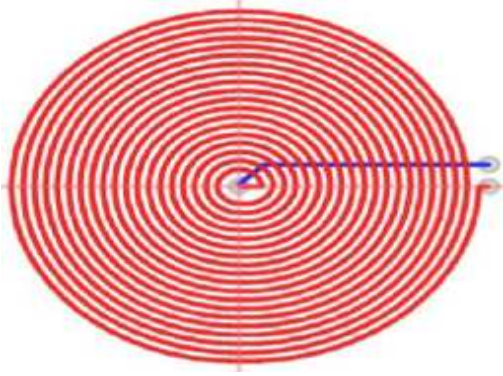
(b) Winding coil

(c) Handmade coil at the end

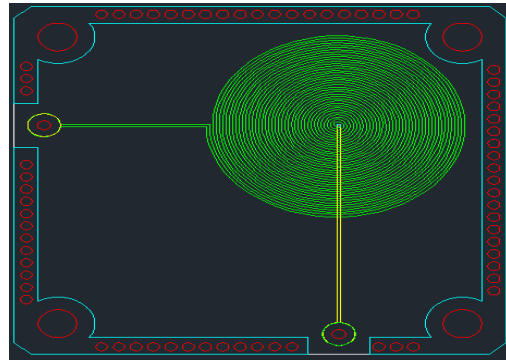
Figure 15. Making a spiral coil with new material. (a) the tip of one end is put into the hole of one plate, (b) wrapping coil while the plates are held down, (c) hand-made coil

In making a coil to have enhanced inductance, the first method was implemented with 2 flat-squared boards with the coil wrapped manually, as shown figure 16. With 2 flat and squared plates, one end of the wire is put into the hole that is located at the center of the plate. The hole allows the combination of two panels on a bolt. The resulting inductance is very close to the theoretically calculated value. Inductance of that coil with 12 to 13 turns wound is about 2.0 – 2.6 μH .

The next issue to be considered was to get coil etched on a PCB.



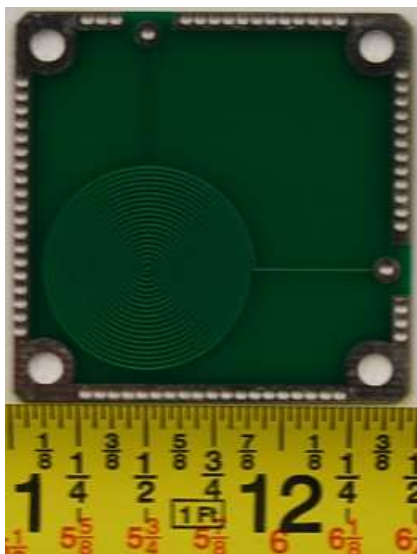
(a) Commercial product in Micro-chip



(b) Coil drawn for study

Figure 16. Drawings of coil for PCB

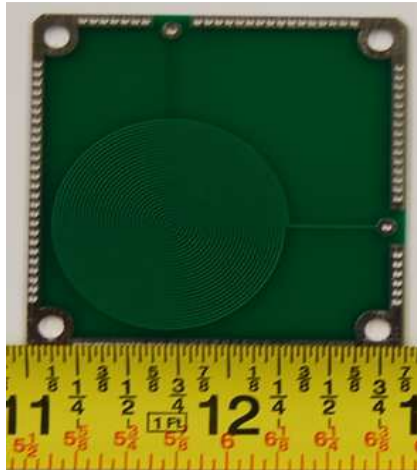
Drawing as shown in figure 17 (b), was completed by drawing a helix with the Pro-E program in 3D and then projected from the top to bottom in 2D Drawings as shown in figure 17, were completed by drawing a helix with the Pro-E program in 3D and then projected from the top to bottom in 2D. The drawing was translated to AutoCAD file format. For experiment, there are 4 different coil patterns drawn to AutoCAD. This is to determine how the number of windings or width of trace influences inductance. Four pictures shown in figure 18 are PCB-based coils made by the “Keum-hyung” Co, of South Korea from our drawings. 1:1 and 2:1 refer to the trace verses space pattern on the PCB.



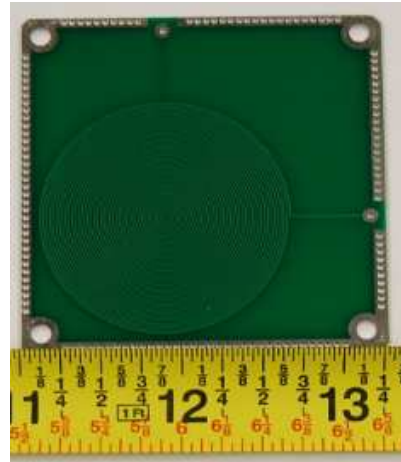
(a) 20 turns(1:1)



(b) 20 turns(2:1)



(c) 30 turns(1:1)

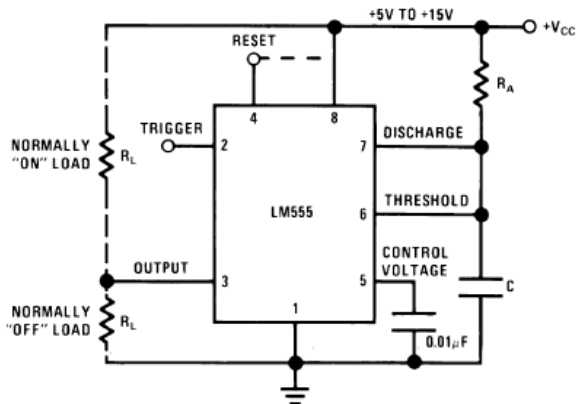


(d) 40 turns(1:1)

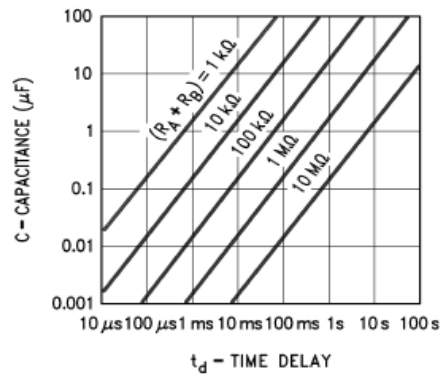
Figure 17. Four etched coils on PCB: (a) ratio of width of trace is 1:1 with 20 turns, (b) 1:2 with 20 turns, (c) 1:1 with 30 turns, d. 1:1 with 40 turns

2.2 Current generator

Vibrators for general purpose includes: 555 timers, crystal vibrators, and multi- vibrator with op-amp. In order to have coil excited, a decent clock is needed. In addition, it has to allow enough current to be drawn to coil. The 555 timer is a popular and general purpose timer, more so than the multi-vibrator because it is simple to build a circuit and easy to apply it to the circuit shown in figure 19.



(a) circuit of 555 timer



(b) response to capacitance

Figure 18. Timer 555 [14]: (a) circuit for application, (b) relationship between capacitance and time delay

The timer 555 is applicable to many clock driven applications like PWM, or a wave transformer, but this device just produces 15 mA as maximum current [14]. As aforementioned, current should be over at least 50 mA [4]. Otherwise the device is not suitable to excite the coil, various kinds of oscillators were tested to find the best one. Programmable generators were tested for this application as well. But the results were somewhat similar to the VCO type clock generator. They had in common the same strange curve forms with the shape of signals not a uniformed square form, but distorted waves.

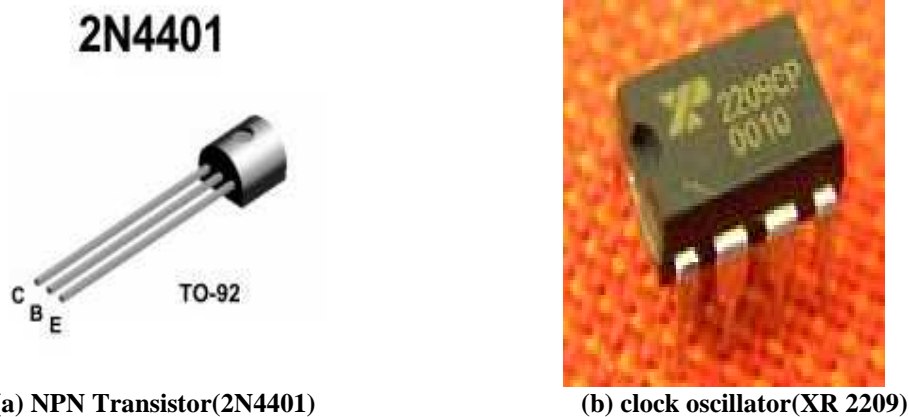


Figure 19. Devices for current generator circuit: a. transistor for current, b. a clock generator to the base terminal of NPN transistor

The reason for this comes from the necessity for impedance match to coil circuit when they were connected [9]. In order to match impedance and ensure sufficient current [9], something is needed between a vibrator and coil circuit. The solution was to use NPN transistor that compensate for the difference in impedance.

For the input to the base port, amount of current from collector to emitter can be controlled by the resistance. The expected amount of current from the collector to the emitter determines the value of the resistor connecting the input to the base port. The most applicable transistor hookup is “common emitter type” that grounds emitter terminal [15]. Therefore, clock pulse provides the base terminal with +5 volts, or 0 volts, allowing current to flow down coil. The

2N4401 transistor (manufactured by Philips) was selected for this study because it can accept 400 mA up to 750 mA. Switching time is about 580 nsec (equal to about 1.7 MHz). Considering required current (over 50 mA), and the clock source (1MHz), the 2N4401 was well suited to be used. In the circuit, the current flow is determined by 2 resistors, one is connected to collector, the other to emitter [15]. This pulsed clock produces sine wave like output across the coil because of the low pass filter. A XR2209 voltage controlled oscillator in figure 21(b) (produced by EXAR co), is applied to the base terminal of the NPN transistor in order to clock out 1MHz.

2.3 Passive Low-pass filter

To remove noise above the 1 MHz-signal, a low-pass filter was applied after the coil. In other words, for an RC circuit, the voltage across coil is detected and amplified. Before amplification, ambient signals on top of the main signal must be filtered out. The capacitance for the cutoff frequency is determined by the following equations.

$$F_c = \frac{1}{2\pi RC} \quad (4)$$

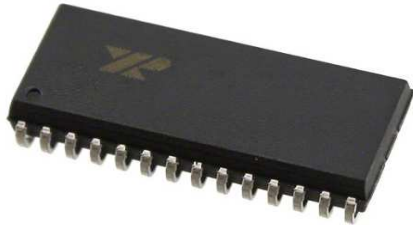
So if $R = 159 \Omega$ and $F_c = 1\text{MHz}$,

$$C = \frac{1}{2\pi R F_c} = \frac{1}{2\pi(159)(1 \times 10^6)} = 1.0 \times 10^{-9} \quad (5)$$

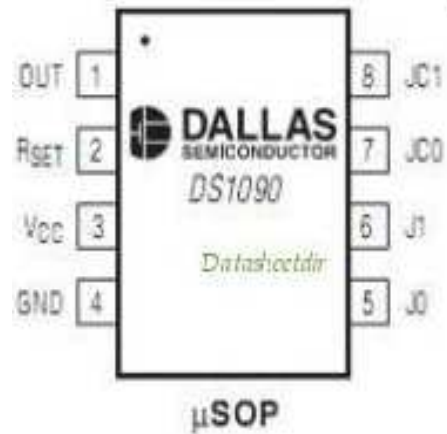
The signals after being filtered out look smoother than before when probed with the HP 54601A oscilloscope.

2.4 Analog to Digital conversion with a sampling clock generator

There are two types of ADC's, serial and parallel, to be considered. With the Propeller and Basic Stamp microprocessors serial ADC's are limited due to timing problems when reading a large number of sensors. Typically the robotic foot many have as many as 10 sensors or more to provide the needed data for rough terrain walking.



(a) XRD 8785



(b) DS 1090

Figure 20. Devices to be used for analog to Digital conversion: (a) ADC in 8bit parallel, (b) 7MHz clock generator

With a parallel ADC there is no need for synchronization, sampled data can be transferred to the I/O ports of a microprocessor at fast rate. The XRD 8785 in figure 21 (a) is 8bit parallel ADC, with an external system clock. The sampling frequency can be chosen by the designer because the ADC refers to an external clock not the microprocessor. Without the sync part in assembly code [refer to the code in Appendix D], data is read up to the speed of 1.2 MHz, which is measured directly by the HP 54601A oscilloscope.

The DS1090 clock generator from Dallas Semiconductor for 7 MHz, up to 8MHz, was used as an external clock. It was stable, but generated additional noise in the circuit board. Through a variety of experiments, the DS1090 noise was easily handled by the use of a potentiometer. The analog potentiometer is attached to the control port with a 3.3 voltage regulator. With this addition the DS1090 provided the clock port of the XRD 8755 ADC with a stable 7 MHz rate.

At 7MHz the XRD 8775 ADC can pick up 7 data points along the signal wave that is running at 1MHz. These 7 data points are enough to reliably determine the peak point among them. The Propeller accepts 8 bit data in parallel at the rate of 1.2 MHz. This is one sixth slower

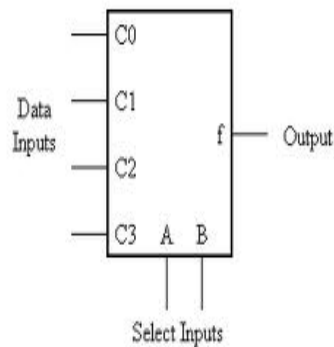
than the external clock speed of 7 MHz. The technique used was to read the XRD 8755 ADC values 7 times for one sensor coil. So with the Propeller reading data at 1.2 MHz the net sensor sampling rate, with 7 readings per sample, comes to 171.43 KHz. Therefore the system throughput rate with 10 coil sensors is estimated to be 17.143 KHz. The rate is fast enough for the robotic foot to provide useful terrain information for the robot response control system.

2.5 Power management and avoiding redundancy with multiplexers

After confirming that one coil was properly read through the computer, multiple coils were built into a sensor circuit. Simply, each sensor coil circuit was added up onto one main board. The problem that developed was high current flow through the circuit. One circuit of each sensor coil consumed 160 mA, so the current came to about 520 mA for 4 sensor coils. The resolution of the problem of high current draw with multiple sensors was to use a multiplexer and make only one of the coil circuits connect to the clock generator at a time.



(a) ADG608B



(b) Example of multiplexer

Figure 21. Multiplexer: (a) ADG 608 with 8×1 channels (www.ictradenet.com), (b) an example about using mux

In figure 22 (b), based on the selection by A and B, one of the data input, C_0 to C_3 , is linked to the output. The ADG 608 (from Analog Device Co.) in figure 24 (a) was the multiplexer used in this study for the purpose of switching channels.

Two multiplexers were used: one for XRD 8785 ADC, and the other for power. By using the multiplexers only one sensor coil was turned on at a time, limiting current to 160 mA.

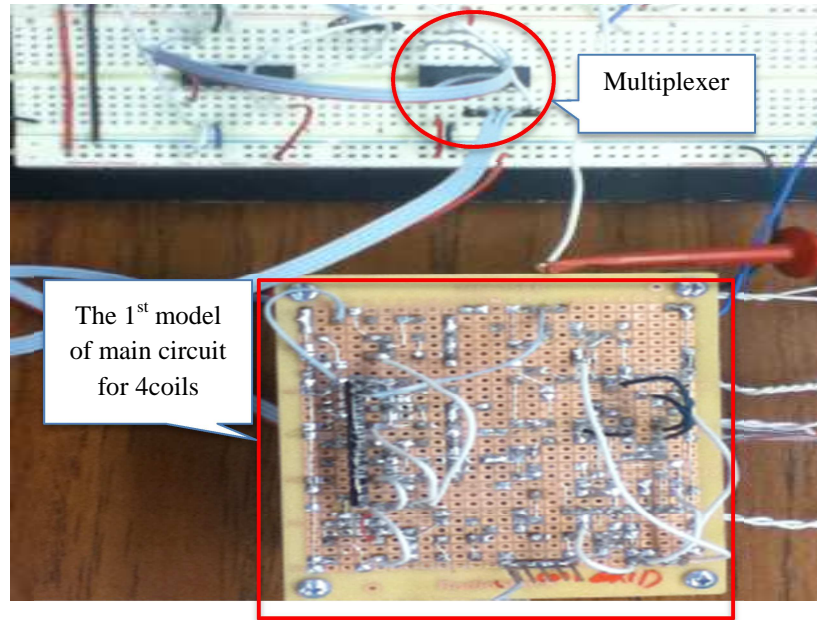


Figure 22. Multiplexer to power source

The control pins of each multiplexer are driven by the microprocessor.

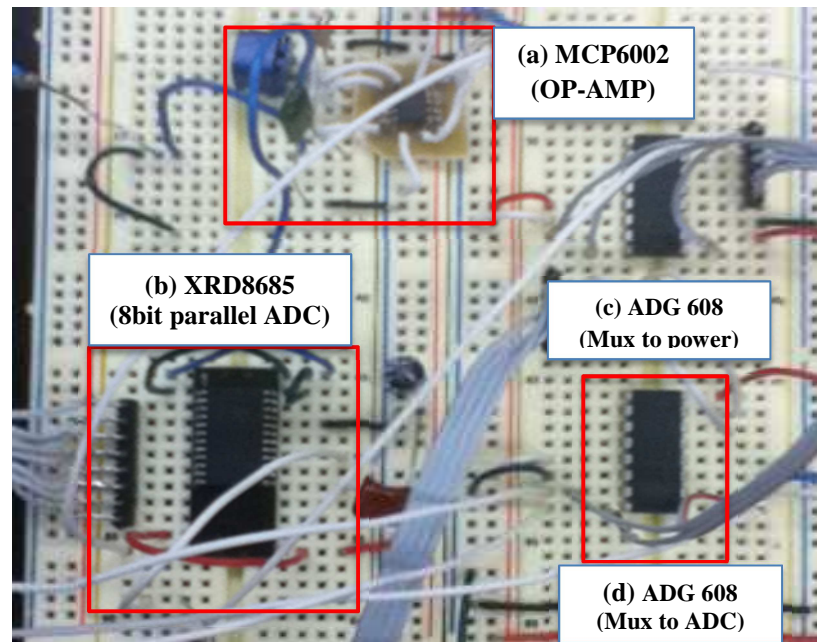


Figure 23. Multiplexer (d) to ADC (b)

2.6 Microprocessor to read ADC

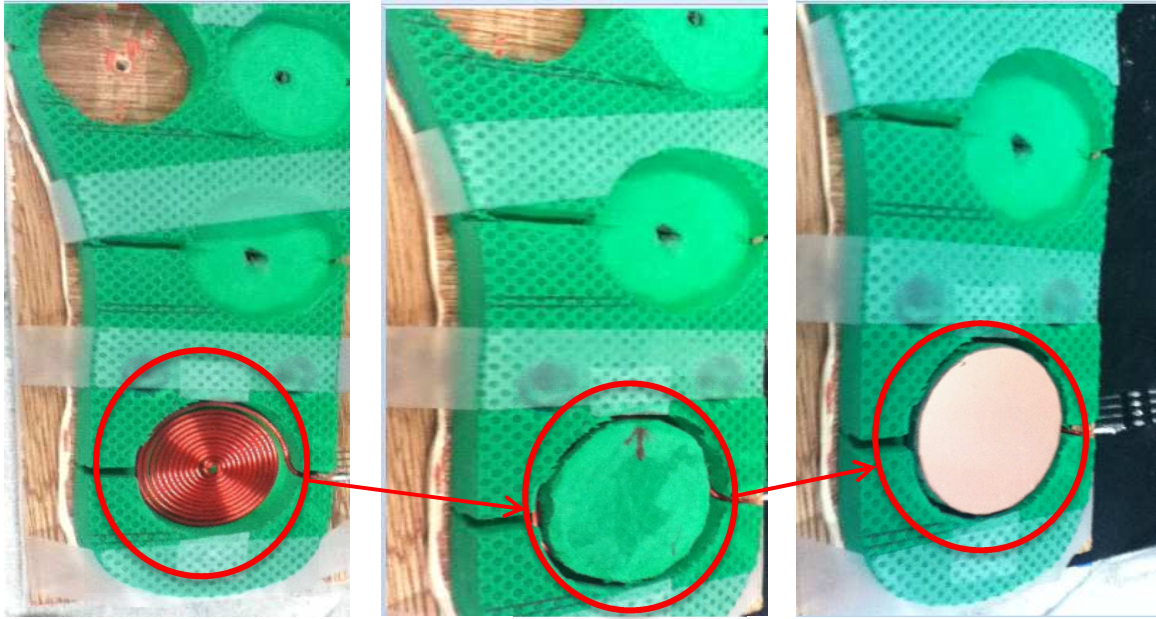
The embedded microprocessor is much cheaper but has limited functions compared to personal computers [17]. For data gathering applications an embedded microprocessor is ideal due to the low cost and small footprint. There is no need for the GHz speeds provided by personal computers used for computation

The Propeller microprocessor used in this study has 8 multiprocessors on one chip, called cogs [19]. Therefore it can work 8 different tasks at a time with only one chip [19]. The Propeller has two programming languages, one called “Spin”, the other “Assembly” [19]. The Spin language is very user friendly but considerably slower than Assembly. Most programs developed for the Propeller have both languages in one code file with assembly used for those functions needing the added speed [19]. Furthermore, the Propeller programming segments can be reused by other Propeller programs like object files in the C++ language [19]. This is the one of the powerful properties of the Propeller microprocessor compared to other processors.

2.7 Test beds for developed sensors.

The initial test bed for the hand wound sensors was a flexible sandal. The sandal was made of polyurethane and was evenly thick and flexible. It was easily carved out and cut out to the form desired as shown in figure 25.

The positioning of the sensor coils on the sandal was determined from a study on gait analysis [20]. Four points were selected on the surface of the sandal to position the handmade sensor coils. The diameter of the hand-made sensor coils was about 1.7 to 2.0 inches. Testing of the sandal showed varied signals by deformation due to the easy movement of the handmade coils.



(a) coil after in a hall

(b) spacer on top of coil

(c) target metal at the top

Figure 24. Sandal with coils as a test bed

The next test bed was made with a rigid panel on which sensors are placed with a few sheets of polyurethane inserted as a gap spacer. The thickness was able to be precisely varied.

3. Troubleshoots

3.1 Interference among coils

With the handmade coils, a circuit was built to hold 4 sensor coils. In the first trial, no problem was observed when the 4 coils were powered at the same time. However, after a multiplexer was applied to decrease the high current flow it was observed that the voltage values across the powered sensor increased when targets were putting on the unpowered sensor coils. It was found that each coil had loops on the same common ground even though only one is turned on. This voltage change phenomenon was explained by “mutual inductance” [8]. This is when one sensor coil creates an electro-magnetic field that induces current in the unpowered nearby sensor coils [8].

The first method tried to correct this problem was isolating non-selected coils from common ground by applying a multiplexer. Based on tests, a sensor coil turned on was not influenced by others that were completely isolated from ground. The datasheet of the ADG 608 shows that it has its own internal resistance of 30 to 40 Ω . That resistance is quite large within this circuitry, because it allowed less current to flow through the sensor coil to change the pattern of signal. In addition, the multiplexer did not make coils cut off completely.

Another try was to use a multiplexer for the input clock to base terminal of NPN transistor. This was not a solution to the problem, because it also could not isolate other coils from the one enabled.

The last revision was to put the multiplexer right before coils from the main clock source. The multiplexer has resistance before flowing current down through the sensor coil. With one single multiplexer, the circuit was totally isolated from others. However, the multiplexer resistance was 40 Ω and it needed to be lowered to 20 Ω , to make an appropriate amount of

current flow through the sensor coil. The simple solution was to connect 2 multiplexers in parallel, which brought the resistance down by half. It turned out that the parallel connection ensured better signals.

Chapter 4. Test and results

The test results are based on the developed setup conditions.

4.1 Coil tests

The number of winding	Coils on PCB			Hand-made coils		
	20	30	40	13	14	
Width of Trace(inch)	.01	.02	.01	.01	.032	.032
Space between traces(inch)	.01	.01	.01	.01	.039	.031
Calculated L(uH)	2.67	4	9	21.33	2.604	2.881
Measured L(uH)	2.2	3.6	7.5	20.4	2.0	2.6

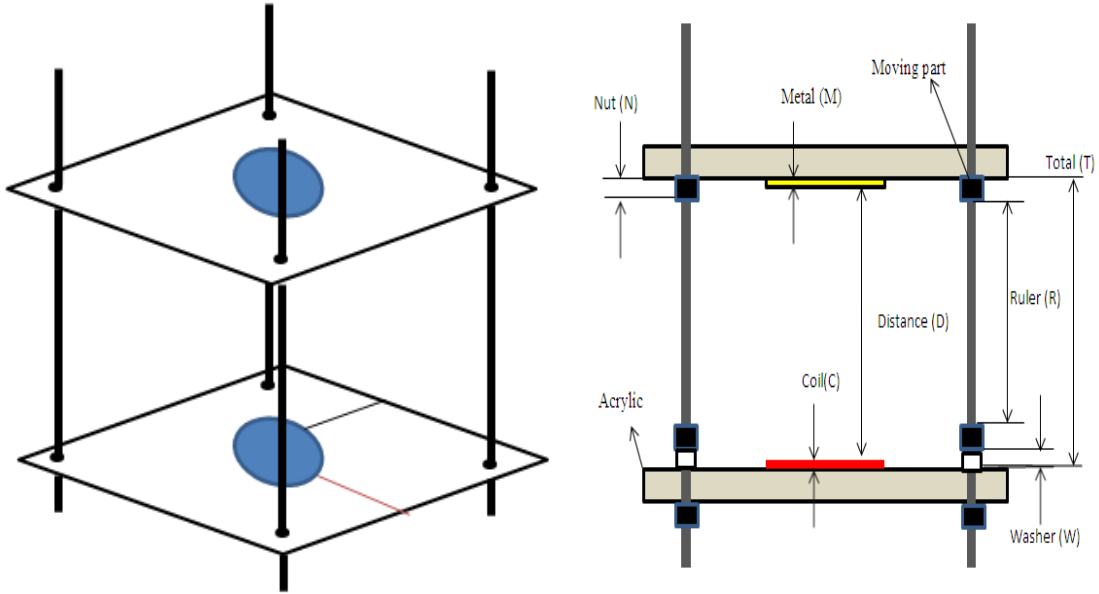
Table 2. Measured inductance versus calculated one

Table 2 indicates that calculated inductance with the formula introduced in the chapter 2 is close to the measured figures. Therefore, the formula can help designers predict the inductance of a coil. The hand-made coils also show values close to the calculated numbers.

The coils made by hand are unstable due to a variety of conditions such as vibration, inaccurate placement, irregular space between coils and deformed coils. These factors make the inductance of the handmade coils changeable and unstable. Contrarily, the PCB coils have accurate and constant geometry so the signals from them are clear and stable.

4.2 Measurement of each coil

To measure the characteristics of the coils in various patterns, a new tool, shown in figure 28, was required for testing them.



(a) 3D view of the measurement tool

(b) Side view of the measurement tool

Figure 25. A measurement tool for coil: (a) 3D view, (b) Side view of the tool

In figure 26 (b), the distance (D) is measured with a caliper at each point. Therefore, the actual distance when the upper nuts are adjusted is

$$\begin{aligned}
 D &= R + (N - M) + (N + W - C) \\
 &= R + 2N + W - (M + C)
 \end{aligned}
 \tag{7}$$

R is measured with a caliper whenever D is changed. Table 3 is the thickness of the various components in the test tool.

Comp.	Handmade Coil	PCB		Nut	Washer	Metal
		Coil	Cover			
Thickness (Inch)	0.052	0.044	0.044	0.126	0.043	0.062

Table 3. Thickness of components

The graph in figure 27 shows the voltages versus gap distance for one of the handmade coils.

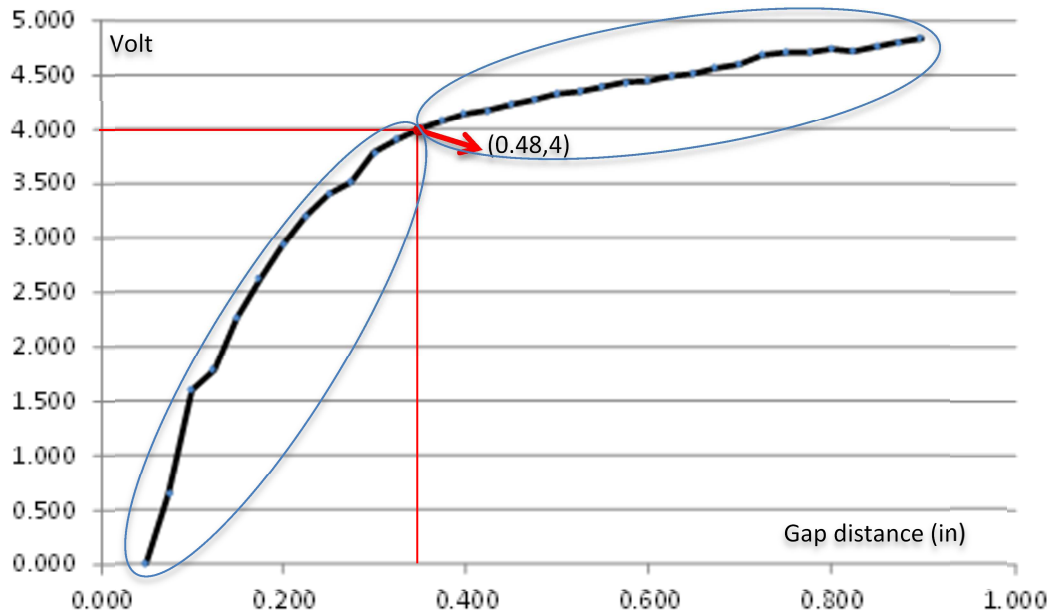


**Figure 26. The Characteristic curve of the hand-made coil of voltage to depth.
The resistance attached to emitter is 10 Ω .**

The curve above shows that the handmade coil has two relatively linear sections breaking at the point (0.35, 4). This was the first graph to prove the good potential of the coil as a sensor.

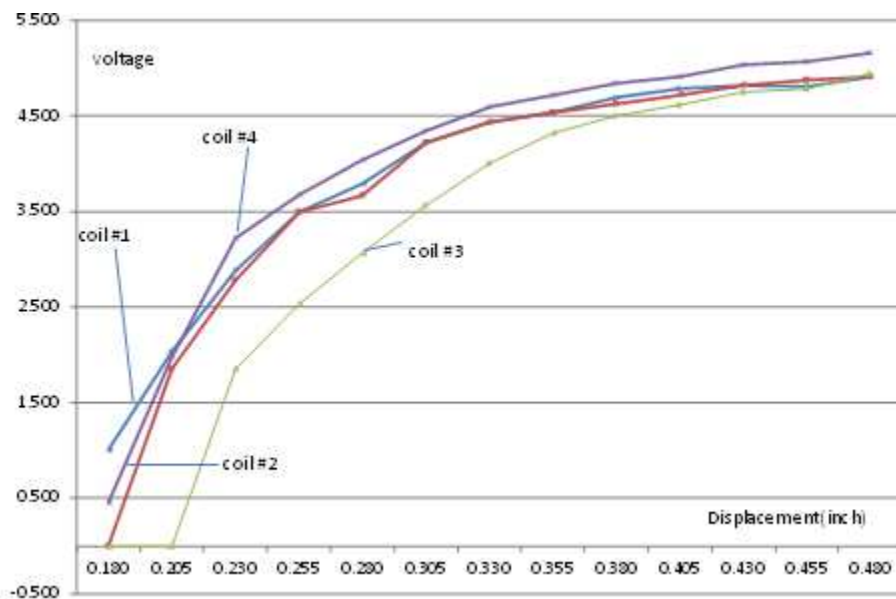


Figure 27. curves for 4 handmade coils with 13 turns wound to be set up on sandal(1st test bed).

The figure 28 shows voltages of 4 different handmade coils for every displacement. Overall the 4 curves are very similar to that in figure 27. The 3rd one was quite low value as compared to the others. Initially, it is believed that the winding direction caused to drop voltage values based on the backward wrapping direction [21]. However, the reason for the 3rd one having a voltage that was a bit lower than the others originated from interference and was solved by isolating the coils which were not selected.

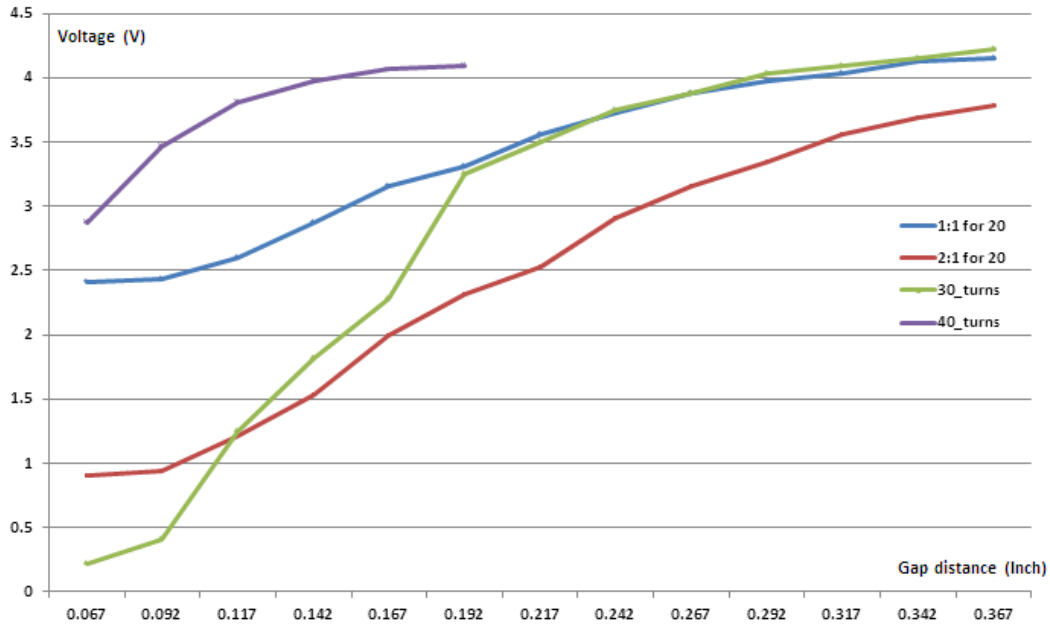


Figure 28. 4 coils etched on PCB after removing interference. The blue color is the coil with 20 and ratio of trace width to space of 1:1. The red is with 20 turns and ratio of 2:1. The green is a coil of 30 turns and ratio of 1:1. The last one is a coil with 40 turns and a ratio of 1:1. These curves were repeatable based on 3 tests.

In figure 29, experiments were carried out after having solved the interference problem by isolation of all coils. When the blue and red coils are compared, the only different condition is the ratio of trace to space. The coil with 2 to 1 ratio has better characteristics than one with 1 to 1.

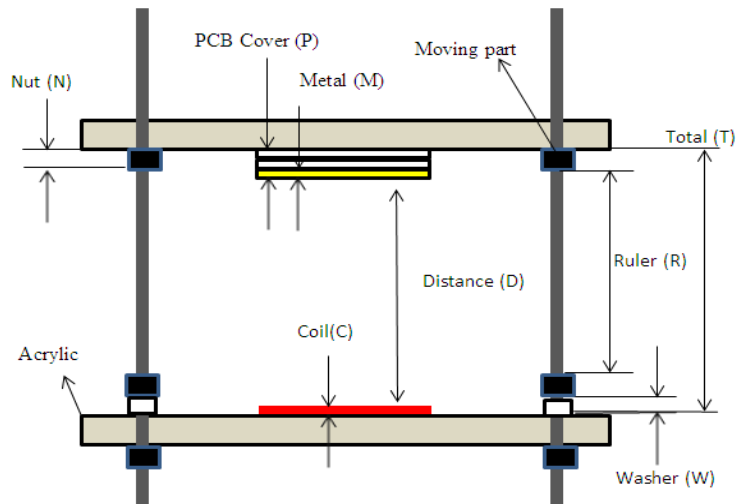


Figure 29. PCB Cover (P) is added to the previous setup

Conclusions and Recommendations

In summary, the new robotic touch foot sensor was inspired by the idea of the inductive touch sensor developed by Microchip. Based on the RLC circuit theory, the coil sensor can detect the variant signal due to the gap distance between the coil and conductive metal.

The gap spacer which gives the sensor elasticity to absorb the impulsive force, is determined by what the maximum expected force will be caused by the robotic gait. From the simulation with ADAMS program, it is calculated to 108 lb-force on the steel for Jay-Walker. This number can be used as a reference to determine the thickness and the stiffness of the spacer in the future.

The other aspect that was addressed is how to make coil, and what the inductance for each pattern would be. With the given formula, inductance can be calculated with good accuracy. Even with the handmade coils, the inductance was close to the value prescribed by the formula.

When developing this sensor there was one major problem that had to be solved. This was the interference between coils. This was solved by placing multiplexer right before input of each coil.

The next major testing needs to be to fabrication and testing of the sensor on the Jaywalker robot. This testing should include the development of a robust flexible covering and mounting for the foot. The other possibility to be considered is that this sensor can be extended for robotic fingers, to sense pressure while holding or touching an object. The foreseeable obstacle is in solving how to magnify signal across a small coil with only 3 or 5 turns.

References

1. Co, H., *ASIMO technical information as an education material*, 2007, Honda Co.
2. Suwanratchatamane, K., M. Matsumoto, and S. Hashimoto, *Haptic Sensing Foot System for Humanoid Robot and Ground Recognition With One-Leg Balance*. Ieee Transactions on Industrial Electronics, 2011. **58**(8): p. 3174-3186.
3. Strunk, G., *Parallelized Distributed Embedded Control System for 2D Walking Robot for Studying Rough Terrain Locomotion*, 2010, University of Kansas.
4. Inc., M.T., *mTouch™ Inductive Touch User's Guide*, 2009.
5. Wikipedia, *Eddy Current*.
6. Stoll, R.L., *The analysis of Eddy Current*, 1974, Clarendon Press, 1974.
7. Mayergoyz, I.D. and W. Lawson, *Basic electric circuit theory : a one-semester text*1997, San Diego: Academic Press. xiv, 449 p.
8. Johnson, D.E. and D.E. Johnson, *Electric circuit analysis*. 3rd ed1997, Upper Saddle River, N.J.: Prentice Hall. xiv, 848 p.
9. Wentworth, S.M., *Fundamentals of electromagnetics with engineering applications*2005, Hoboken, NJ: John Wiley. xx, 588 p.
10. *Inductance calculator*.
11. Hoeschele, D.F., *Analog-to-digital and digital-to-analog conversion techniques*. 2nd ed1994, New York: J. Wiley. xiii, 397 p.
12. Lewis, F.L., *Applied optimal control & estimation : digital design & implementation*. Prentice Hall and Texas Instruments digital signal processing series1992, Englewood Cliffs, N.J.: Prentice Hall. xxiv, 624 p.
13. Steele, R., *Delta modulation systems*1975, New York,: Wiley. x, 379 p.
14. Semiconductor, N., *LM 555 Timer*, 2006.
15. Jaeger, R.C. and T.N. Blalock, *Microelectronic circuit design*. 2nd ed2004, New York: McGraw-Hill Higher Education. xxv, 1506 p.
16. Semiconductor, P., *2N4401 NPN switching transistor*, 2004.
17. Instruments, T., *ADS7888*, 2005, Texas Instruments Incorporated.

18. Short, M., M.J. Pont, and J.Z. Fang, *Assessment of performance and dependability in embedded control systems: Methodology and case study*. Control Engineering Practice, 2008. **16**(11): p. 1293-1307.
19. MacKenzie, I.S., *The 8051 microcontroller*. 3rd ed1999, Upper Saddle River, N.J.: Prentice Hall. x, 366 p.
20. Lindsay, A., *Propeller Education Kit Labs version 1.1*, Parallax Inc.
21. Whittle, M., *Gait analysis : an introduction*. 4rd ed2004, Oxford ; Boston: Butterworth-Heinemann. x, 220 p.
22. Horowitz, P. and W. Hill, *The art of electronics*. 2nd ed1989, Cambridge England ; New York: Cambridge University Press. xxiii, 1125 p.

Appendix A: Flowchart of the robotic touch foot sensor

Appendix A contains the flowchart that shows how the robotic touch foot sensors are working. Under the tree, it needs 4 parts to have all sensors working. Each of them has detailed functions.

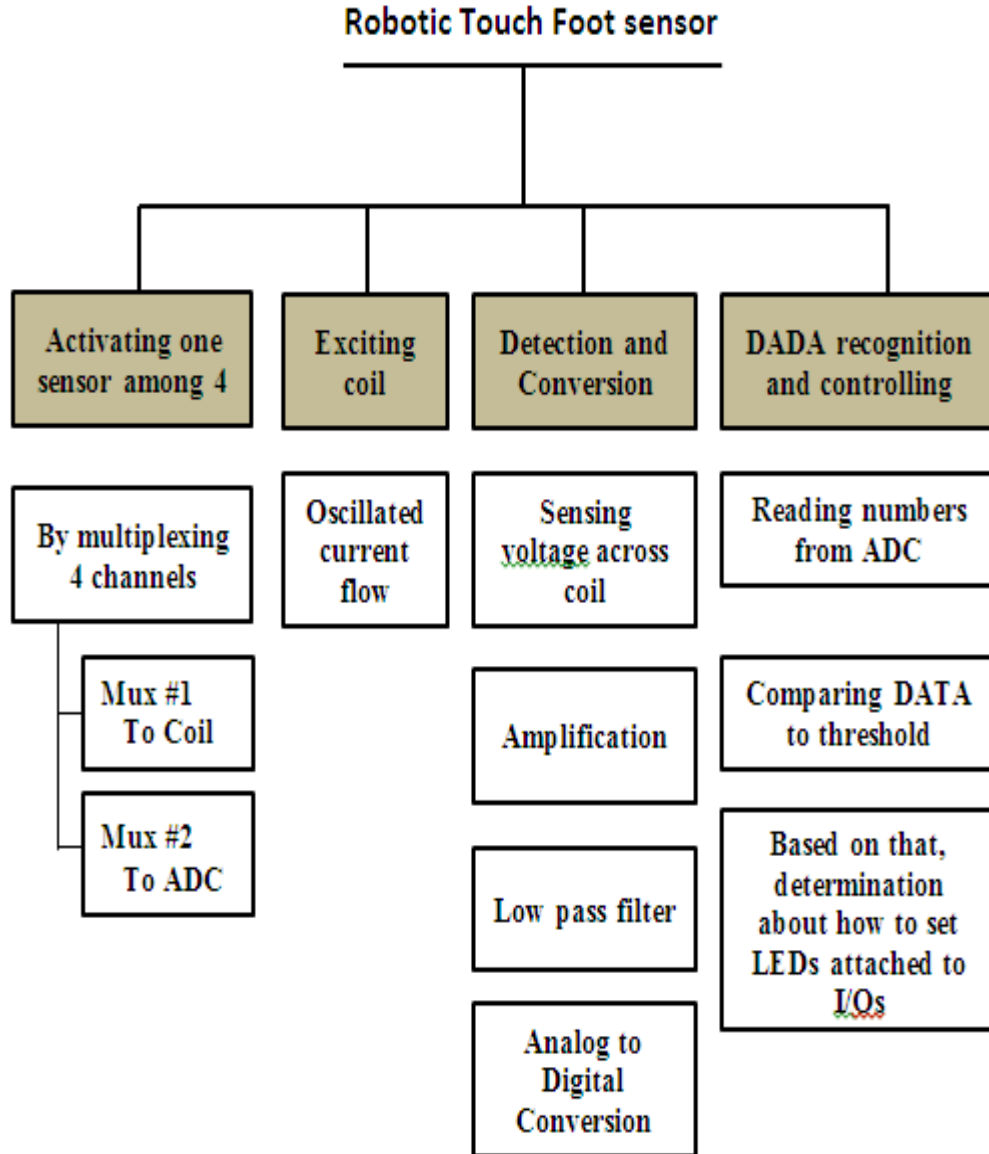


Figure A.1 Flowchart of the robotic touch foot sensor

Appendix B: Schematics for the robotic touch sensor circuits

Appendix B contains the wiring schematics for each of the first trial circuit, 2nd circuit and the last version of circuit, which includes 2 multi-vibrators, coil wiring with multiplexers and an Op amp.

Appendix B.1 The first circuit for the robotic touch foot sensor

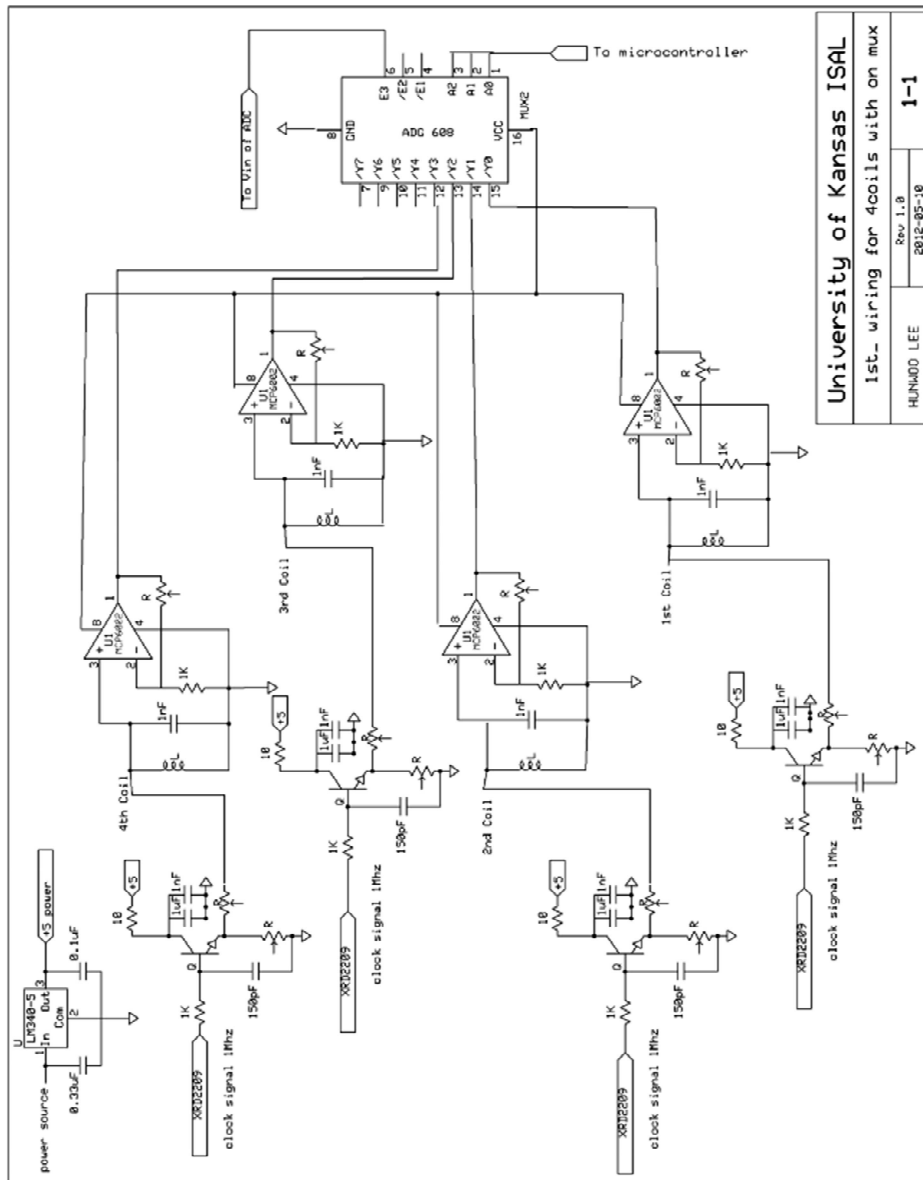
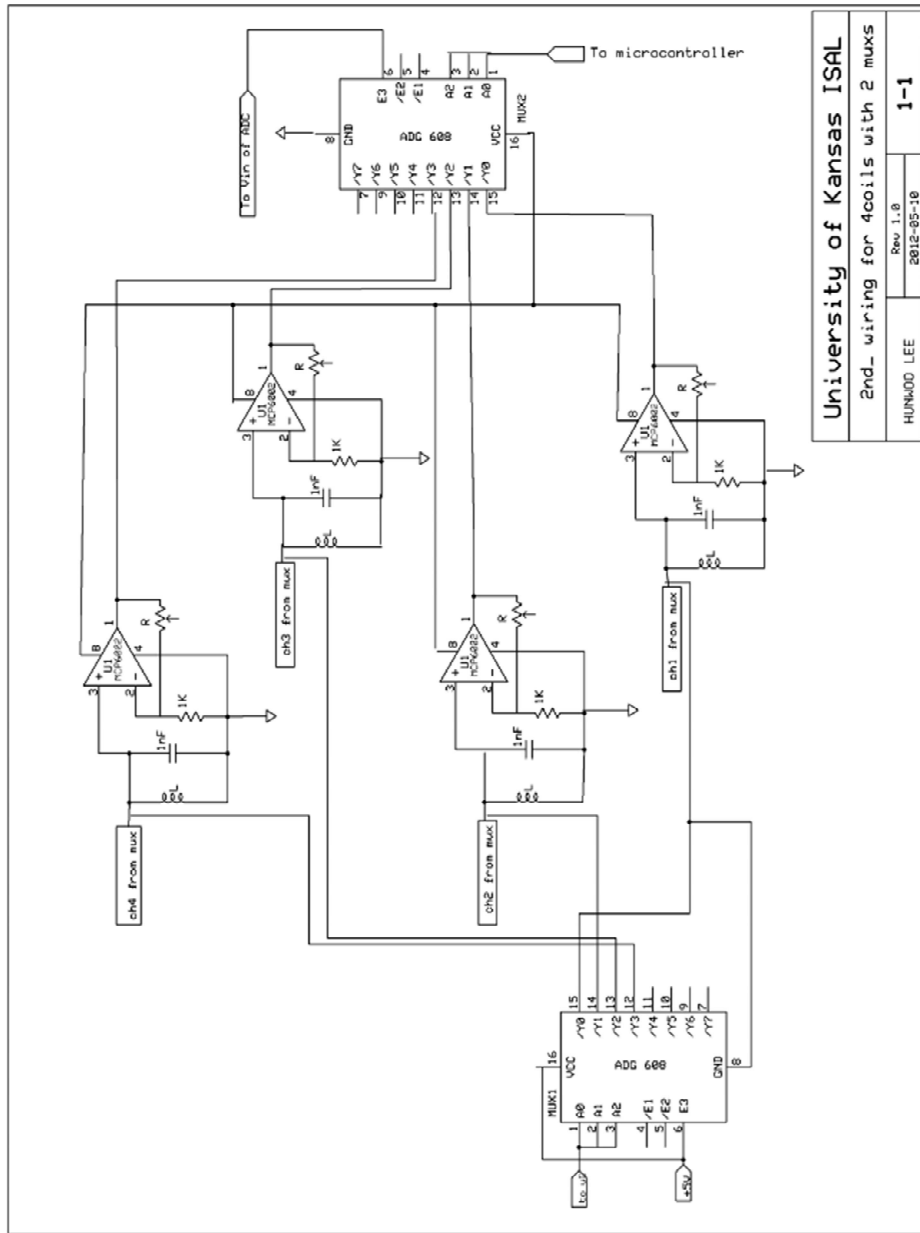


Figure B.1 The first circuit to test sensors without selecting one of sensors. It consumes .53A with 4 coils turned on.

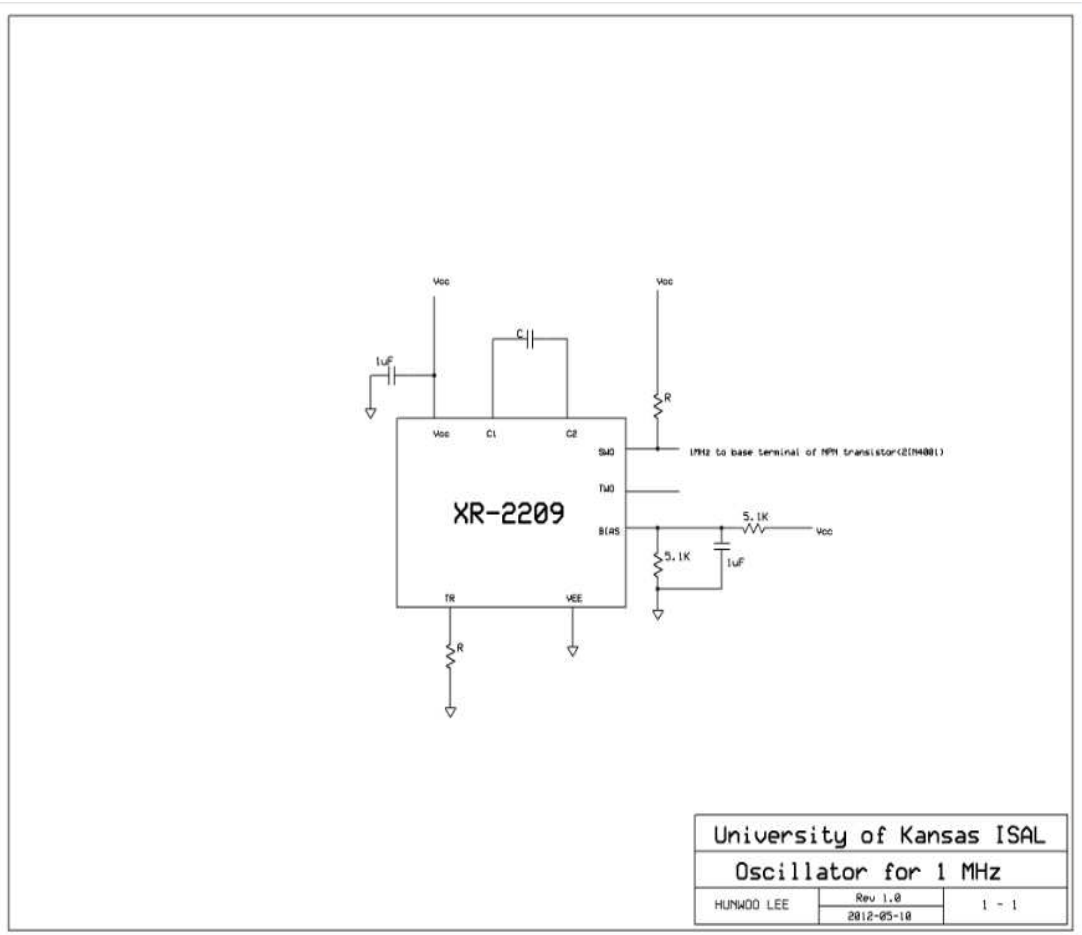
Appendix B.2 The second version of the sensor circuit



University of Kansas ISAL
 2nd_wiring for 4coils with 2 muxs
 Rev 1.8
 HUNKOO LEE
 2012-05-10
 1-1

Figure B.2 The 2nd circuit to solve power consumption with a multiplexer. The multiplexer acts to select one of sensors turned on at a time.

Appendix B.3 1MHz vibrator to NPN Transistor



B.4 7MHz vibrator to ADC

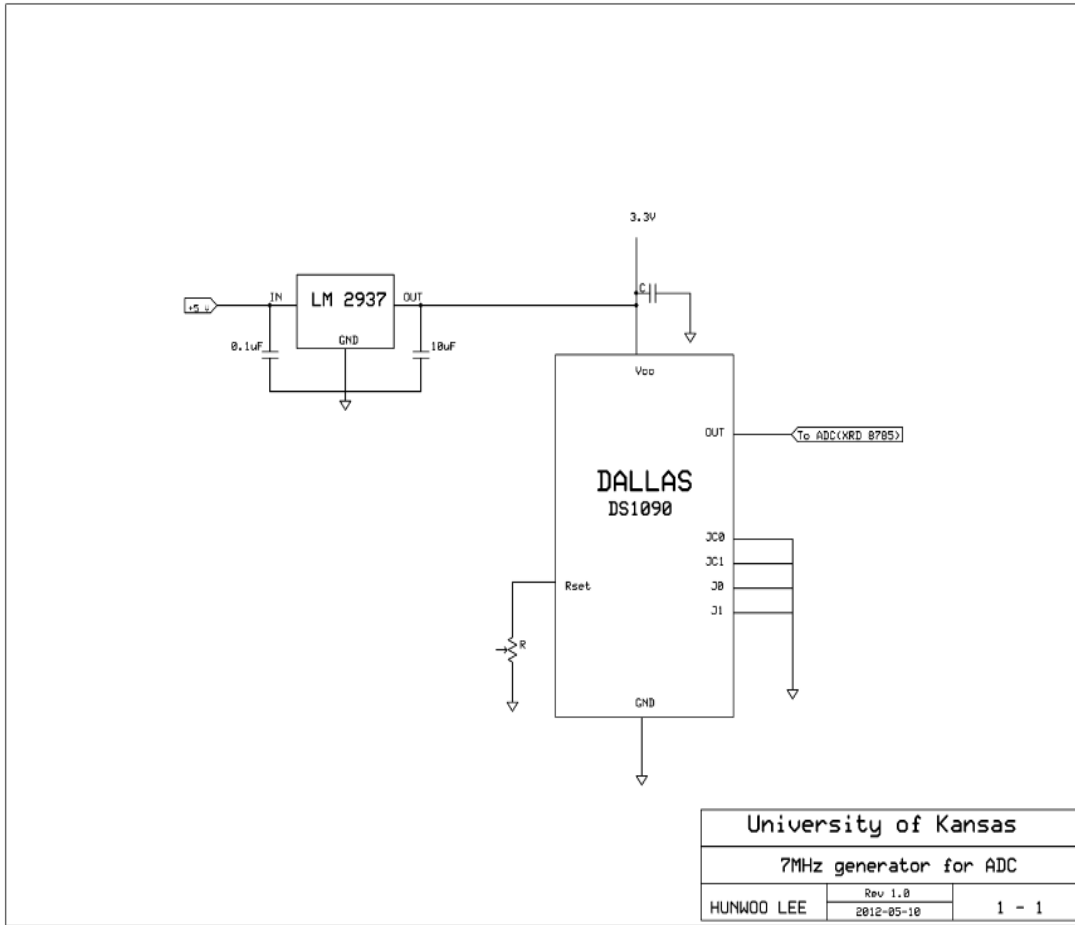
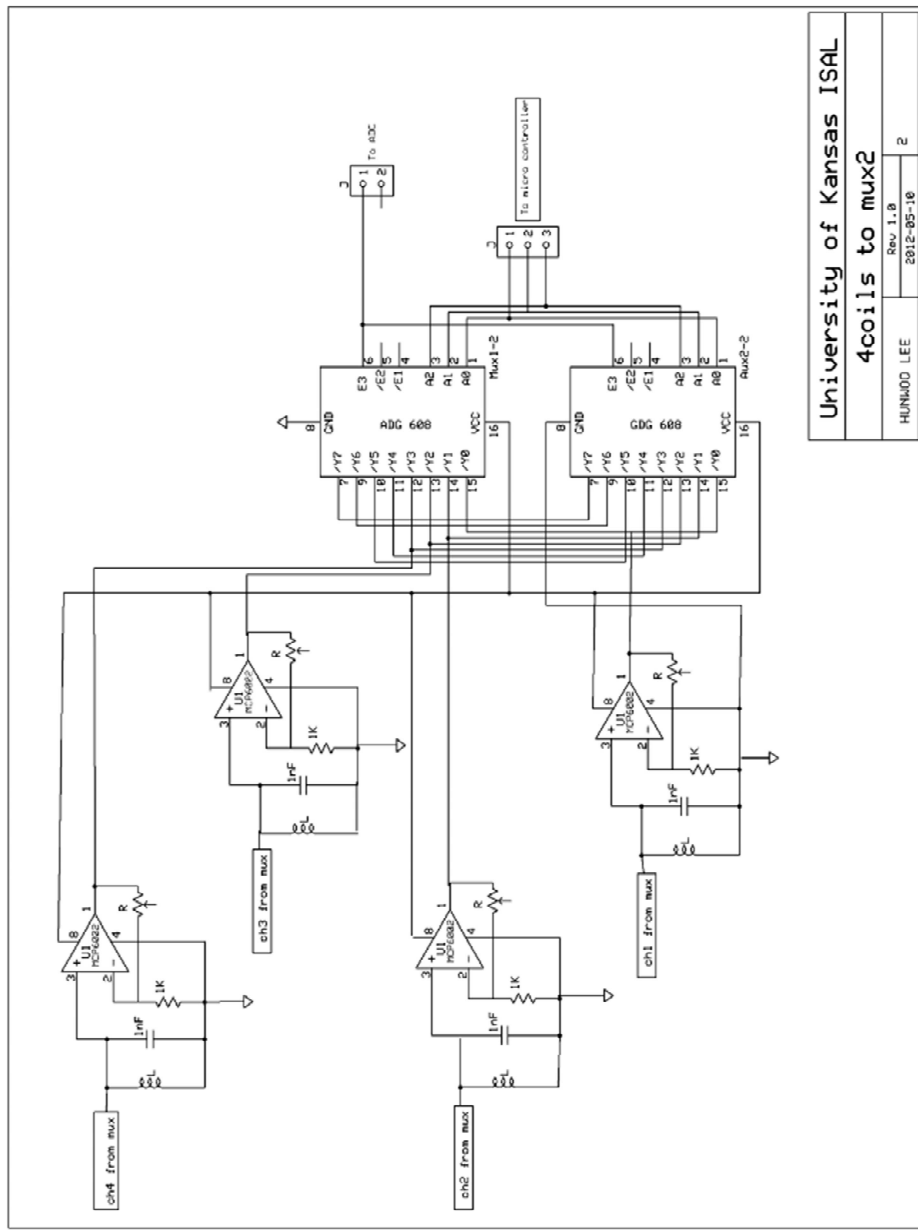


Figure B.4 7MHz multi-vibrator to be used for ADC as sampling clock.

B.5 Diagram for 4 coil circuits with 2 multiplexers



University of Kansas ISAL	
4coils to mux2	
HUNHOD LEE	Rev. 1.0
	2012-05-10
	2

Figure B.5 Wiring diagram between Op-Amp and multiplexers connected to input of ADC.

B.6 Wiring diagram for ADC setup to microprocessor

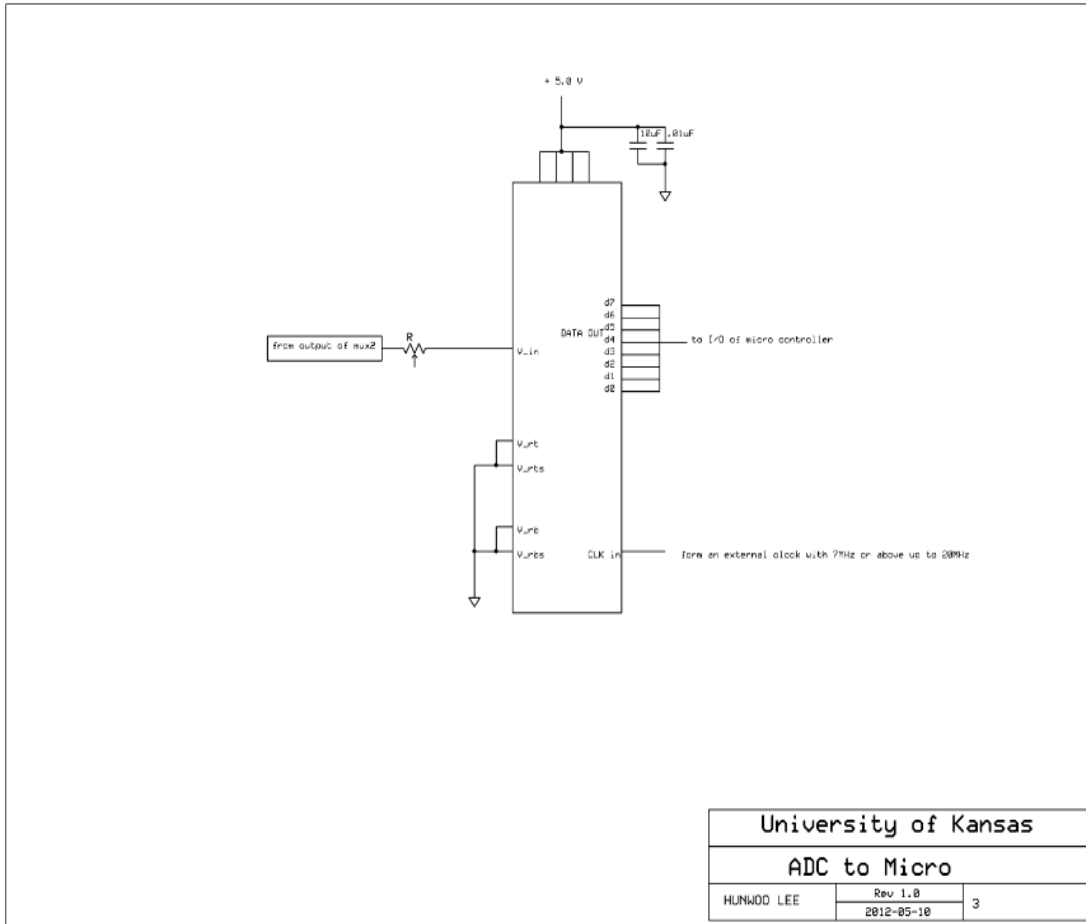


Figure B.6 Wiring diagram for ADC to micro controller and the output of 4 Op-Amps.

B.7 Wiring diagram for excited current driver with a multiplexer

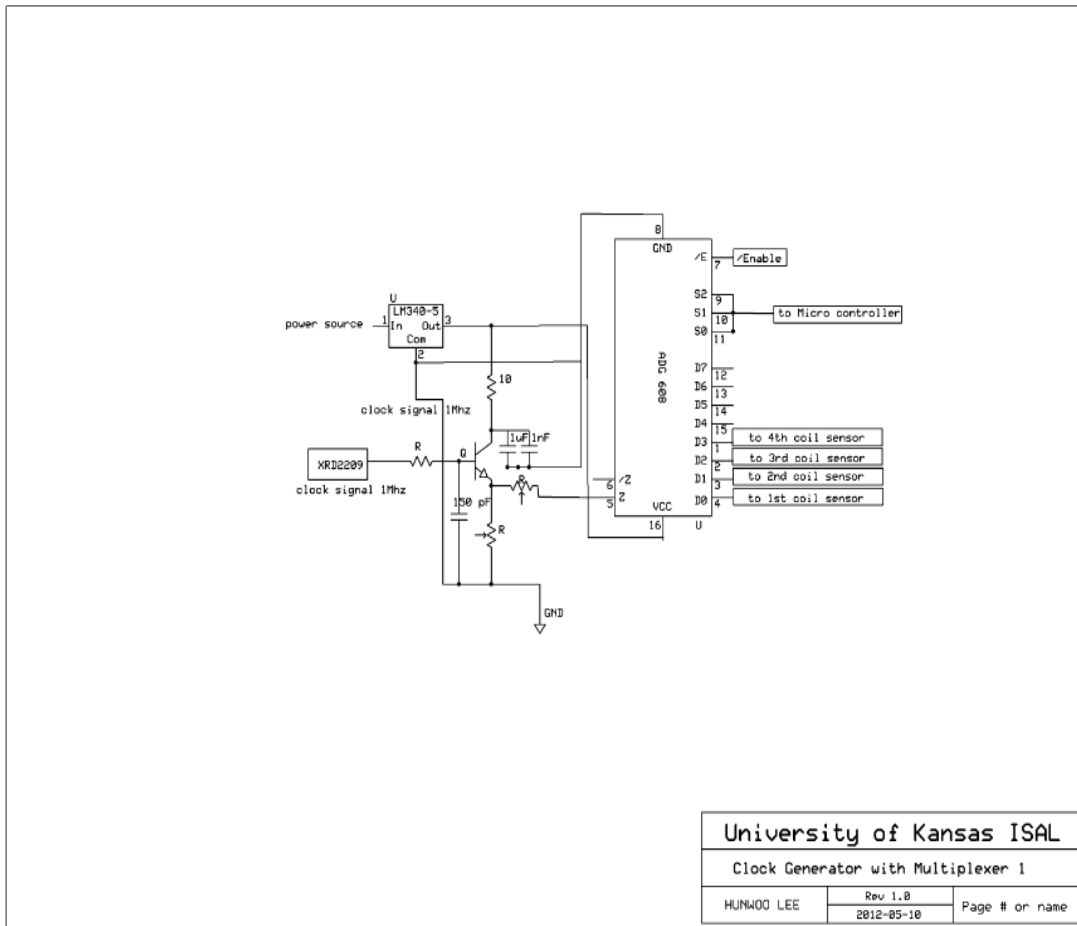


Figure B.7 Clock generator with a current driver and multiplexer to separate one coil from others against interference.

B.8 Wiring diagram for test board

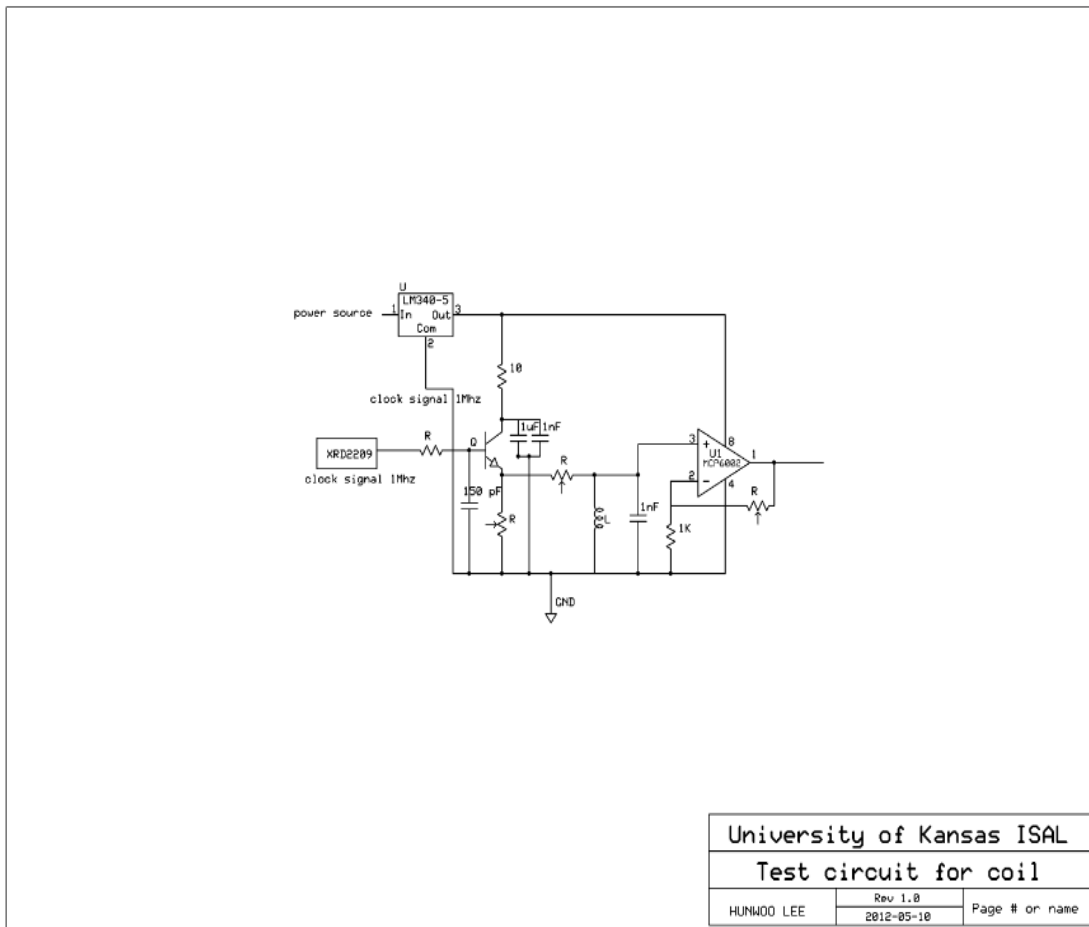


Figure B.8 Test board for various experiments. Before building up a circuit, it is tested first on this board.

Appendix C: Interference among coils

Appendix C describes how the interference occurs among coils.

The first experiment on mutual interference was carried out like the setup below.

Appendix C.1 The first test about mutual interference at the beginning

a. Schematic for test

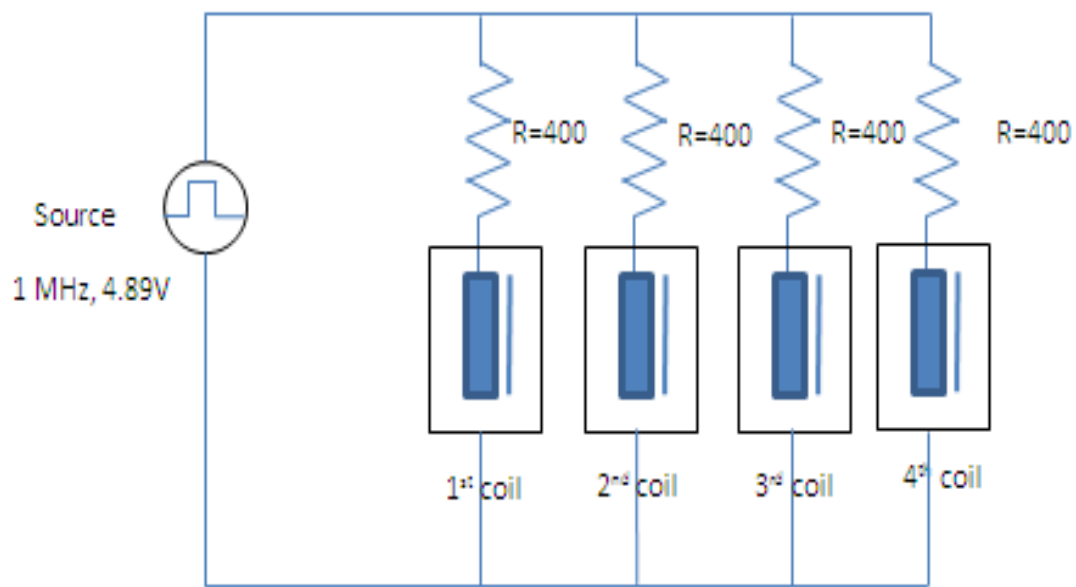
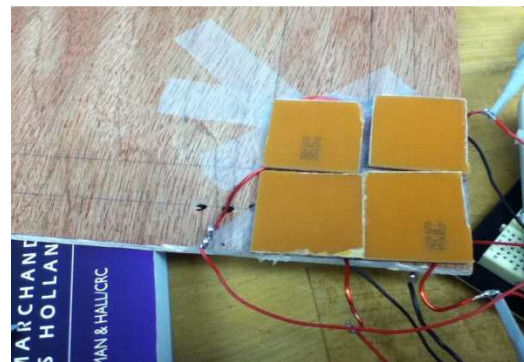
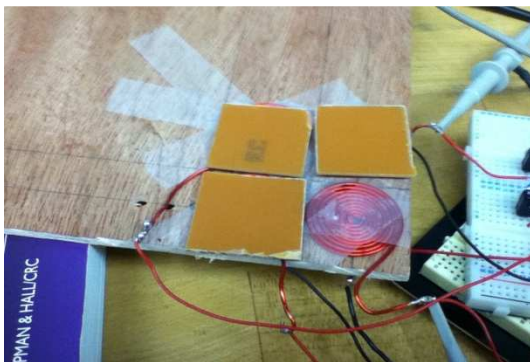
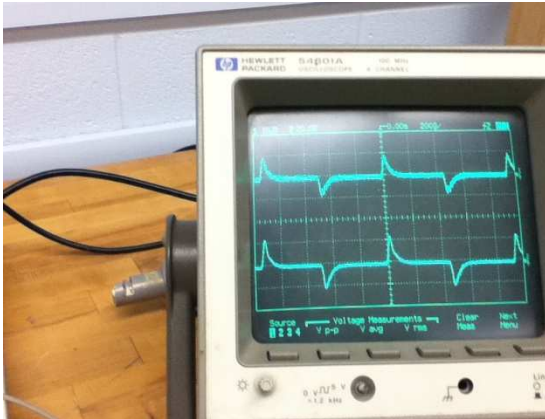


Figure C.1 Setup wiring diagram for testing

b. Setup for measurement

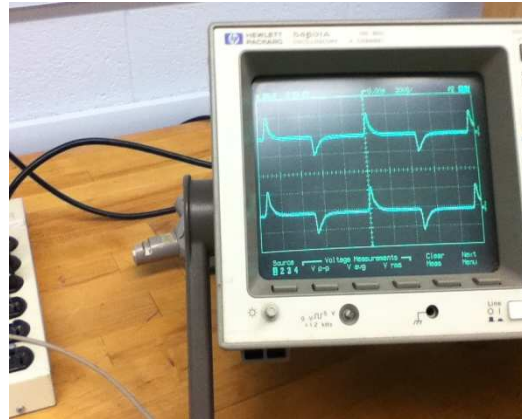


(a) One coil only is opened



(c) signals through oscilloscope from (a)

(b) All coils are closed



(d) signals from (b)

Figure C.1.1 pictures above shows how to conduct the test. (c) is a signal from (a) setup, (d) from (b)

c. Result

Open / closed		Voltage with one metal on dark cell				Metals put on coil in order				
coil	origin	1 st coil	2 nd coil	3 rd coil	4 th coil	1 st metal	2 nd metal	3 rd metal	4 th metal	
1	Open	1.122	1.210	1.116	1.097	1.084		1.116	1.119	1.113
	Closed	0.687	0.675	0.694	0.684	0.681		0.684	0.697	0.697
2	Open	0.963	0.972	0.966	0.972	0.962	0.972		0.953	0.947
	closed	0.561	0.534	0.525	0.525	0.525	0.534		0.534	0.538
3	Open	0.728	0.725	0.734	0.728	0.719	0.725	0.734		0.728
	Closed	0.375	0.372	0.378	0.363	0.378	0.372	0.381		0.384
4	Open	0.723	0.722	0.728	0.725	0.734	0.722	0.719	0.709	
	closed	0.336	0.334	0.334	0.336	0.336	0.334	0.334	0.338	

Table C.1 pictures above shows how to conduct the test. (c) is a signal from (a) setup, (d) from (b)

d. With the table, all coils did not show serious problem with interference. But the values from coils were not amplified by Op-Amp. With the result, it was believed that there was no interference among coils. This caused the problem that is mentioned earlier.

Appendix C.2 The second test for interference

1. Testing interference of the setups below and the signals on HP oscilloscope

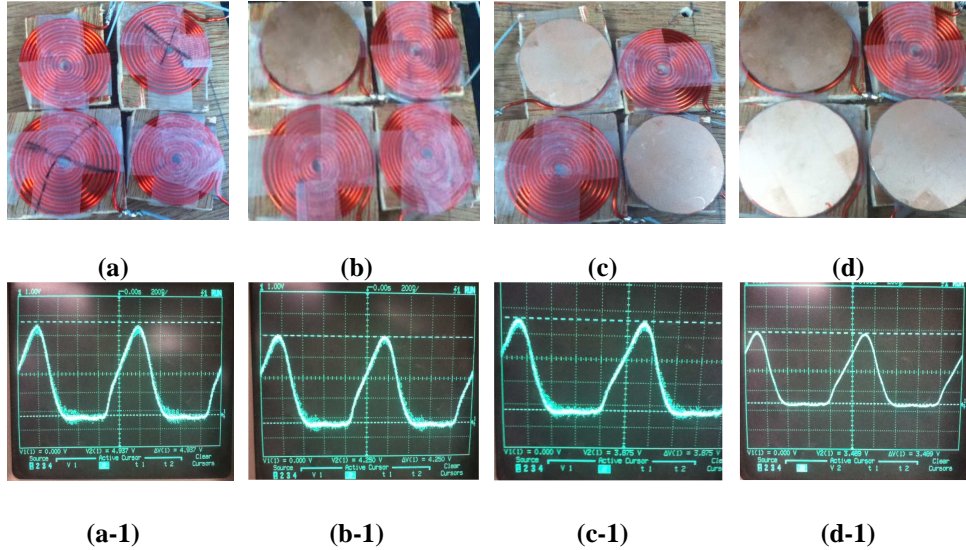


Figure C.2.1 Testing interference among coils. The circuit diagram is introduced in Appendix B.2

2. Result: As shown in figure, the signal is getting lower than the previous one because it has one more piece of metal. The effect of distance among coils was tested again, but it had nothing to do with the interference. This is the reason why a multiplexer must be applied to the coils like the figure B.3.5.

Appendix D: Programing codes for robotic touch foot sensor working

Appendix D includes the final program in the Propeller. As explained before, it has two languages: assembly, spin. The assembly is used to read the ADC at 1.2MHz. And the Spin code is to analyze what the values are and simply displays what they are with LEDs.

```
con
```

```
  _clkmode = xtal1 + pll16x
```

```
  _xinfreq = 5_000_000
```

```
var
```

```
  long data[100]          'for spaces to store values read by adc
```

```
  long gap                'for just in case
```

```
  byte temp[100]         'buffer to resotore the values from data space
```

```
  byte tmp                'temporarily space to swap long type data to byte
```

```
obj
```

```
  serial : "FullDuplexSerial"
```

```
pub start | idx,i,f,g
```

```
  serial.start(31,30,0,115200)
```

```
  idx := 0                'idx ==> point to locate one of arrays
```

```
  tmp :=0                 'tmp
```

```
  dira[9..8]~~~
```

```

    dira[15..12]~~          'outputs determined by micro processor after reading
values
    outa[15..12]~          ' clear them to zeros
    outa[9..8]~
    waitcnt(clkfreq*3 + cnt)

    cognew(@go,@data)      'New cog to read sampled values from

repeat                    '7 times repeat for reading:
    outa[9..8]:=00
    repeat until idx == 10
        temp[idx] := data[idx]    ' Swap long to byte
        if (temp[idx] > 90)      ' from 255-90, set threshold as 90. above 90, it is
recongized as 1
            i++                  'if it is over 90, count i up with 1
            idx++                'Increment for memory location

        if(i>2)                  'counted value is great than 2,
            outa[12]~~          'just turn the LED connected to pin 12
        else
            outa[12]~          'if not, set pin 12 to zero
            i:=0
            idx:=0
    'waitcnt(clkfreq/10000 + cnt)
    outa[9..8]:=01

```

```

repeat until idx == 10

temp[idx] := data[idx]    ' Swap long to byte

if (temp[idx] > 80)      ' from 255-90, set threshold as 90. above 90, it is
                        ' recongized as 1

i++                      'if it is over 90, count i up with 1
idx++                    'Increment for memory location

if(i>2)                  'counted value is great than 2,
outa[13]~~              'just turn the LED connected to pin 12
else
outa[13]~               'if not, set pin 12 to zero
i:=0                    'after finishing one procedure, clear i and idx to make them
                        'jump to the first location

idx :=0

'waitcnt(clkfreq/10000 + cnt)

outa[9..8]:= %10

repeat until idx == 10

temp[idx] := data[idx]    ' Swap long to byte

if (temp[idx] > 80)      ' from 255-90, set threshold as 90. above 90, it is
recongized as 1

i++                      'if it is over 90, count i up with 1
idx++                    'Increment for memory location

if(i>2)                  'counted value is great than 2,
outa[14]~~              'just turn the LED connected to pin 12

```

```

else
    outa[14]~          'if not, set pin 12 to zero
i:=0                  'after finishing one procedure, clear i and idx to make them
                      'jump to the first location
idx :=0
outa[9..8]:= %11
repeat until idx == 10
    temp[idx] := data[idx]    ' Swap long to byte
    if (temp[idx] > 90)      ' from 255-90, set threshold as 90. above 90, it is
                              'recongized as 1
        i++                  'if it is over 90, count i up with 1
        idx++                'Increment for memory location

    if(i>2)                  'counted value is great than 2,
        outa[15]~~          'just turn the LED connected to pin 12
    else
        outa[15]~          'if not, set pin 12 to zero
i:=0                    'after finishing one procedure, clear i and idx to make them
                      'jump to the first location
idx :=0

```

DAT

```

    org    0

```

go

```

        mov     addr,par    'reading point address that is the first space of the array

        andn   DIRA,pinmask1

set1    mov     t1, #10    ' reading 7 times per one coil

        mov     t2, addr   'to reuse the point address, store it to t2

read1   mov     value,ina  'Reading a value from 8bit I/O

        wrlong  value,t2   'Write the value to the place that the pointer is pointing
at
        add     t2,#4      'Increase the address with 4 because of the long variable.

        djnz   t1,#read1  'Jump to read1 unless t=0, everytime, t = t-1

        jmp    #go

```

```

pinmask1  LONG    $000F
pinmask2  Long    %1111_00000000

addr      res    1
value     res    1
t1        res    1
t2        res    1
t3        res    1
t4        res    1
t5        res    1
t6        res    1

```

Appendix E: Characteristics of coils

Appendix E has two kinds of data about voltage to gap distances from two different circuits. One from Appendix B.2 shows interference problem. Hand-made coils were used. The other describes the enhanced stability without the problem. The coils etched on PCB were tested.

(a)	coil #1	coil #2	coil #3	coil #4	coil1(metal)	coil3(metal)
0.180	1.000	0.000	0.000	0.444	1.788	0.000
0.205	2.038	1.850	0.000	1.975	2.913	1.225
0.230	2.880	2.788	1.850	3.225	3.444	2.194
0.255	3.500	3.500	2.538	3.683	3.850	2.663
0.280	3.788	3.663	3.069	4.037	4.225	3.288
0.305	4.225	4.225	3.569	4.350	4.440	3.756
0.330	4.442	4.442	4.006	4.600	4.631	4.006
0.355	4.537	4.537	4.319	4.725	4.787	4.287
0.380	4.694	4.631	4.506	4.850	4.881	4.412
0.405	4.787	4.725	4.622	4.912	4.912	4.725
0.430	4.819	4.819	4.756	5.037	4.975	4.850
0.455	4.811	4.881	4.787	5.069	(b)	
0.480	4.912	4.912	4.944	5.162		

Table E.1 the data were measured by the tool in Figure 28. (a) data from 4 coils. (b) test to compare 1st coil and 3rd coil to see why the 3rd coil had small values from the other.

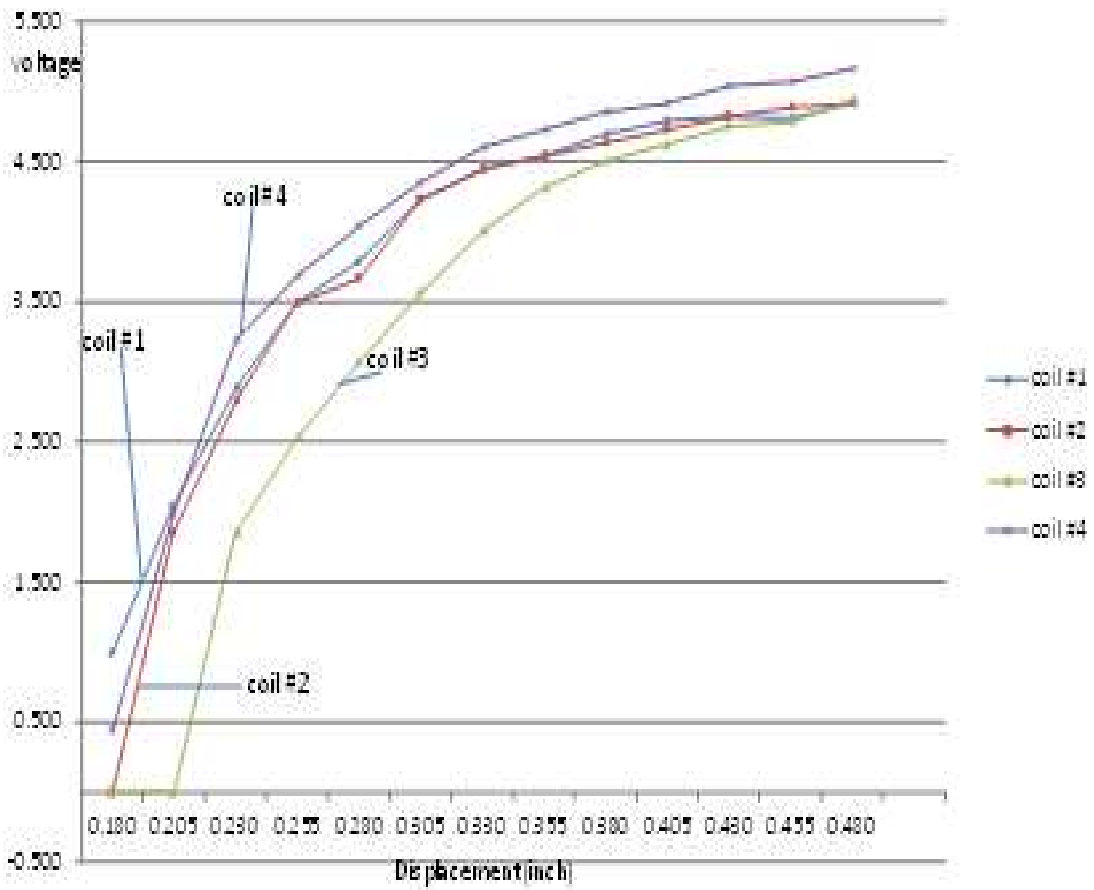


Figure E.1 4 curves from table E (a)

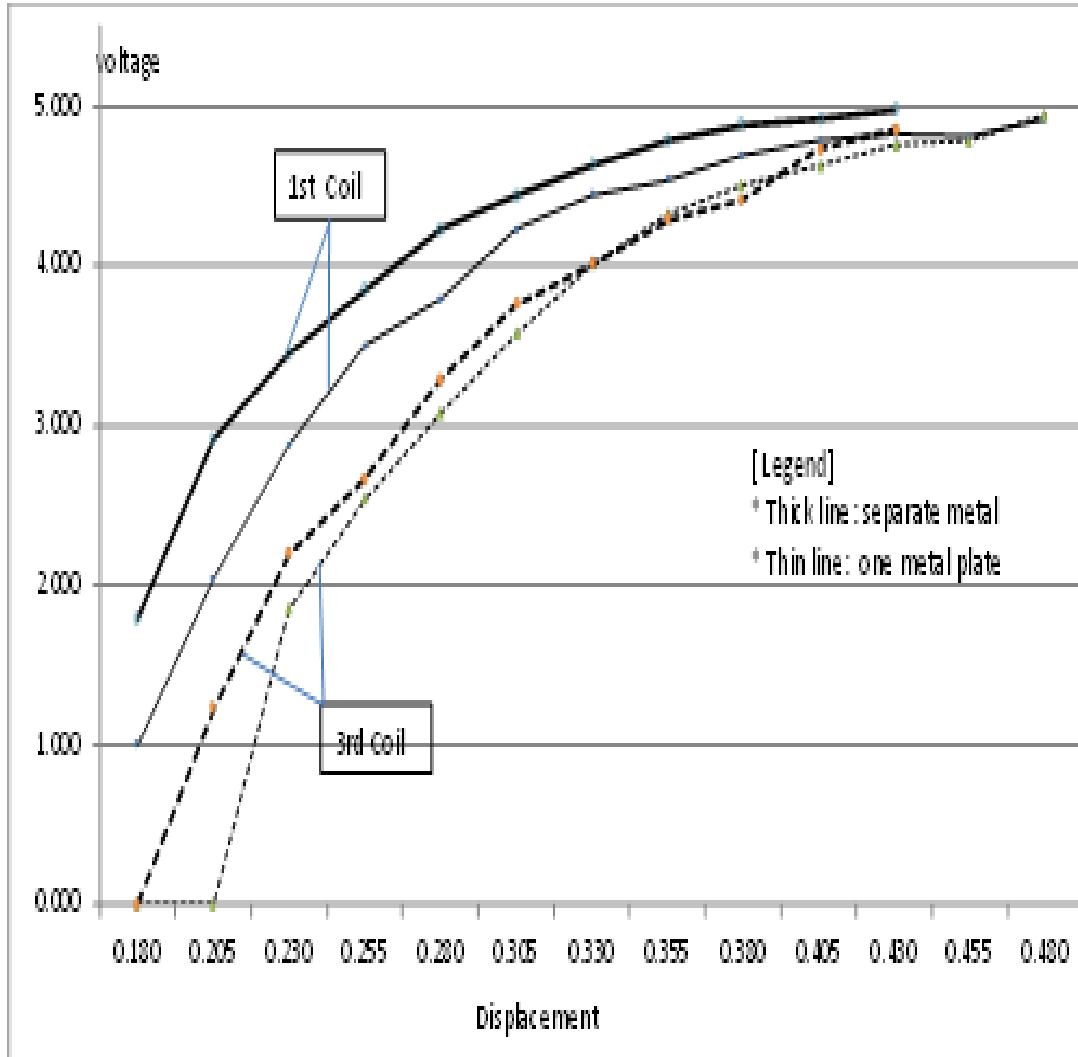


Figure E.1 4 curves from table E (b): the metal was changed from one big plate to two pieces to see if it changed that difference. As a result, it had a little effect on that but not much.

	1:1 for 20	2:1 for 20	30 turns	40 turns
0.067	2.406	0.906	0.218	2.875
0.092	2.438	0.938	0.406	3.469
0.117	2.594	1.219	1.25	3.813
0.142	2.875	1.531	1.813	3.969
0.167	3.156	2	2.281	4.062
0.192	3.313	2.313	3.25	4.096
0.217	3.563	2.531	3.5	
0.242	3.719	2.906	3.75	
0.267	3.875	3.156	3.875	
0.292	3.969	3.344	4.031	
0.317	4.031	3.563	4.094	
0.342	4.125	3.688	4.156	
0.367	4.156	3.781	4.219	

Table E.2 each column shows voltages to distance. And every coil did not have any interruption from others. The curves are provided in figure 30. 1:1, 2:1 stand for ratio of trace to space.